Science of the Total Environment 720 (2020) 137518

Contents lists available at ScienceDirect

Science of the Total Environment

journal homepage: www.elsevier.com/locate/scitotenv

Changes in microclimate and hydrology in an unmanaged mountain forest catchment after insect-induced tree dieback

Jiří Kopáček [a,b,*], Radek Bače [c], Josef Hejzlar [a], Jiří Kaňa [a,b], Tomáš Kučera [b], Karel Matějka [d], Petr Porcal [a,b], Jan Turek [a]

[a] Biology Centre of the Czech Academy of Sciences, Institute of Hydrobiology, České Budějovice, Czech Republic
[b] University of South Bohemia, Faculty of Science, České Budějovice, Czech Republic
[c] Czech University of Life Sciences, Faculty of Forestry and Wood Science, Prague, Czech Republic
[d] IDS, Prague, Czech Republic

HIGHLIGHTS

- Tree dieback changed the hydrology and microclimate in an unmanaged mountain forest.
- Water input to soils, soil moisture, run-off, air and soil temperature increased.
- Relative air humidity decreased but started to increase together with tree regeneration.
- Climate change increased mean air temperature by 1.6 °C, tree dieback by 1.2 °C more.
- Hydrological changes were small (within 4–20%) compared to the undisturbed forest.

GRAPHICAL ABSTRACT

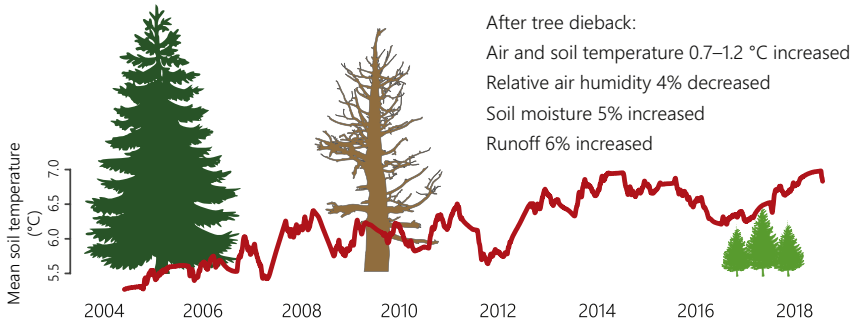

ARTICLE INFO

Article history:
Received 19 September 2019
Received in revised form 6 February 2020
Accepted 22 February 2020
Available online 26 February 2020

Editor: Ralf Ludwig

Keywords:
Bark beetle
Climate change
Spruce forest
Natural disturbance
Microclimate characteristics

ABSTRACT

Hydrological and microclimatic changes after insect-induced tree dieback were evaluated in an unmanaged central European mountain (Plešné, PL) forest and compared to climate-related changes in a similar, but almost intact (Čertovo, CT) control forest during two decades. From 2004 to 2008, 93% of Norway spruce trees were killed by a bark beetle outbreak, and the entire PL area was left to subsequent natural development. We observed that (1) climate-related increases in daily mean air temperature (2 m above ground) were 1.6 and 0.5 °C on an annual and growing season basis, respectively, and an increase in daily mean soil temperature (5 cm below ground) was 0.9 °C during growing seasons at the CT control from 2004 to 2017; (2) daily mean soil and air temperatures increased by 0.7–1.2 °C on average more at the disturbed PL plots than in the healthy forest; (3) water input to soils increased by 20% but decreased by 17% at elevations of 1122 and 1334 m, respectively, due to decreased occult deposition to, and evaporation from, canopies after tree dieback; (4) soil moisture was 5% higher on average (but up to 17% higher in dry summer months) in the upper PL soil horizons for 5–6 years following the tree dieback; (5) run-off from the PL forest ~6% (~70 mm yr^{-1}) increased relatively to the CT forest (but without extreme peak flows and erosion events) after tree dieback due to the ceased transpiration of dead trees and elevated water input to soils; and (6) relative air humidity was 4% lower on average at disturbed plots than beneath living trees. The rapid tree regeneration during the decade following tree dieback resulted in a complete recovery in soil moisture, a slow recovery of discharge and air humidity, but a still insignificant recovery in air and soil temperatures.

* Corresponding author at: Biology Centre of the Czech Academy of Sciences, Na Sádkách 7, 370 05 České Budějovice, Czech Republic.
E-mail addresses: jkopacek@hbu.cas.cz (J. Kopáček), bace@fld.czu.cz (R. Bače), hejzlar@hbu.cas.cz (J. Hejzlar), kucert00@prf.jcu.cz (T. Kučera), matejka@infodatasys.cz (K. Matějka), porcal@hbu.cas.cz (P. Porcal), turek@hbu.cas.cz (J. Turek).

https://doi.org/10.1016/j.scitotenv.2020.137518
0048-9697/

1. Introduction

The number of studies on relationships between forest health and climate has increased during the past two decades due to the accelerating increase of temperature related insect infestation-induced tree mortality in vast areas of European and North American forests (e.g., Anderegg et al., 2012; Mikkelson et al., 2013; Seidl et al., 2017). These studies mostly focussed on climate effects on forest development and the impacts of changes in forest cover on hydrology (e.g., Brown et al., 2005; Wei and Zhang, 2010; Bearup et al., 2014). Information on the effects of natural tree dieback and stand-replacing disturbances on changes in microclimate characteristics (air and soil temperature and moisture) are, however, sparser. The available studies mostly evaluate spatial variability in selected climatic characteristics, comparing their patterns in healthy, naturally disturbed, managed, or clear-cut stands (e.g., Chen et al., 1999; Hais and Kučera, 2008, 2009; Ehbrecht et al., 2019). In general, hydrological and microclimatic variables (particularly solar radiation, air temperature at the ground surface, soil temperature and moisture, throughfall, transpiration, groundwater levels, and discharge) are sensitive to changes in canopy and vegetation characteristics, and exhibit relatively high spatial and temporal variability within a forest (e.g., Chen and Franklin, 1997; Beudert et al., 2007; Bearup et al., 2014; Slinski et al., 2016). Removing tree canopies may result in increasing surface and air temperatures and in decreasing air humidity (Chen et al., 1999; Hesslerová et al., 2018). For example, Hais and Kučera (2008) used thermal remote sensing to determine differences in the surface temperature of spruce forest areas, and observed 5.2 and 3.5 °C increases in clear-cut areas and naturally disturbed stands, respectively, compared to undisturbed stands. Changes in the forest structure and species composition affect water input to soils and run-off (Wei and Zhang, 2010; Caldwell et al., 2016). Most published studies have shown that water discharge from catchments increases when reductions in forest cover by harvesting or natural disturbances exceeded 20–30% (Brown et al., 2005; Beudert et al., 2018; Wei and Zhang, 2010). The elevated water run-off is a net result of decreasing tree transpiration and interception, while increasing soil evaporation and understory transpiration are due to the loss of canopy cover after tree dieback and elevated energy input to (and storage in) the soils (Beudert et al., 2007; Wehner and Stednick, 2017).

One major weakness of many studies on effects of forest disturbances on microclimate patterns is that they do not include pre-disturbance conditions. Long-term empirical data on microclimatic characteristics are especially absent for natural disturbances due to their more stochastic and poorly predictable occurrence than in the case of clear-cuts. Moreover, until recently, disturbed forests have always been salvage-logged in the temperate zone and there was no opportunity to study post-disturbance patterns in non-intervention sites. In the case of surface temperature, this disadvantage can be partly compensated for by evaluating pre-disturbance satellite images in studies based on remote sensing (Hais and Kučera, 2008). This method, however, usually evaluates typical situations during sunny days, thus providing significant differences in surface temperature (and not real differences in air and soil temperature) between individual plots, and may lead to overestimating possible effects. The real effects of natural disturbances on microclimate and hydrological characteristics are very important in models assessing nutrient losses from unmanaged vs. managed forest ecosystems, as well as for knowledge on how forests inherently function (e.g., Aber and Driscoll, 1997; Edburg et al., 2012). Moreover, they can provide a framework within which the impacts of global changes (climate, atmospheric pollution, land-use) on forest ecosystems can be predicted (Houlton et al., 2003).

In this study, we evaluate available data on the microclimatic and hydrological characteristics in two unmanaged mountain forest catchments in the Bohemia Forest (central Europe) obtained over the last two decades. These data were collected as a background for environmental studies focused on the effects of ecosystem recovery from acidification on element and nutrient cycling in soils and waters (Kopáček et al., 2016, 2017), ecosystem modelling (Oulehle et al., 2012, 2019), and reconstructions of historical trends in air temperature (Turek et al., 2014). During our monitoring, a bark beetle outbreak killed most of the mature spruces trees in one of the catchments. We used this unique chance to evaluate the effects of bark-beetle canopy removal on microclimate and water cycle. The aim of this study is to assess changes in air and soil temperature and moisture, water input to soils, and run-off prior to, during, and after tree dieback in the infested catchment, using the intact catchment as a control. Due to the unmanaged regime in these catchments, the following data can be considered as a natural background to all possible management practices and human intervention (including biomass removal or salvage logging) in similar mountain forest areas.

2. Materials and methods

2.1. Description of the study site

Plešné Lake (PL; 13.9 °E and 48.8 °N) and Čertovo Lake (CT; 13.2 °E and 49.2 °N) are situated at elevations of 1087 and of 1027 m, respectively, on the north-eastern slope of the mountain ridge of the Bohemian Forest (Šumava) at the border between the Czech Republic, Austria and Germany (Supplementary information, SI; Fig. SI-1). The areas of PL and CT lakes are 7.6 and 10.7 ha, respectively. The PL and CT drainage areas (catchments including lakes) are 67 and 89 ha in size and are steep, with maximum local reliefs of 288 and 315 m, respectively. The PL and CT catchments are covered with ~0.2 m deep leptosol (38 and 17%, respectively), the rest is dominated by ~0.5 m deep podsol or dystric cambisol (Kopáček et al., 2015, 2017).

In 2000, mountain forest vegetation covered 80–90% of the PL and CT catchments and was dominated by mature Norway spruce (*Picea abies*), with a minor contribution of birch (*Betula pubescens* and *B. pendula*), rowan (*Sorbus aucuparia*), and European beech (*Fagus sylvatica*). Understory vegetation was dominated by blueberry (*Vaccinium myrtillus*), fern (*Athyrium distentifolium*), grass (*Calamagrostis villosa* and *Avenella flexuosa*), and wood-rush (*Luzula sylvatica*) in both catchments (Svoboda et al., 2006; Matějka, 2015).

The unmanaged mature spruce forest was healthy in the PL catchment in 2000, with only a ~7% proportion of dead trees. Most of the PL forest was attacked by a bark beetle (*Ips typographus*) between 2004 and 2008, >80% of original mature spruce trees died in 93% of the PL forest, and only a small area with younger spruce trees survived (Fig. SI-1). Dead trees have been continuously broken by winds during the following years (Kopáček et al., 2015, 2017). All dead biomass has been left on site, because the area is part of the Šumava National Park (declared in 1991). Natural forest regeneration started within 1–3 years after the dieback of adult trees (especially under the parent canopies), when the availability of sunlight on the forest floor increased due to the thinning of dead canopies. This process was rapid (especially at elevations <~1200 m), and the number of spruce seedlings (diameter of crown <0.8 m) increased by an order of magnitude between 2005 and 2015, with average densities of 47 and 670 trees ha^{-1}, respectively (Kopáček et al., 2017); for an example of these changes see Fig. SI-2. The biomass of understory vegetation, especially blueberry, increased after the tree dieback (Matějka, 2015).

The CT forest was almost intact in 2000 and was affected by windthrows in 2007 and 2008, which broke most of the trees along the south–western ridge of the catchment (Fig. SI-1). Other relatively small patches with broken trees and the following bark beetle outbreak occurred in the northern part and throughout the whole CT catchment in 2007–2011. Altogether, the total area of damaged forest (with >50% dead trees) in the CT catchment increased from ~4% to 18% from 2000 to 2011 (Kopáček et al., 2016). Another windthrow uprooted most trees in a relatively small area of western ridge of the CT catchment in October 2017.

2.2. Research plots

Three permanent research plots were established in both catchments for measurements of precipitation (or throughfall), air and soil temperature, and soil moisture. Bulk precipitation (BP) was sampled in open areas without trees at elevations of 1087 (PL-BP) and 1180 m (CT-BP) in the PL and CT catchment, respectively. Throughfall plots were located in flat areas beneath mature Norway spruce trees (~150 years old) at low (L; <1122 m; PL-L and CT-L) and high (H; ~1330 m; PL-H and CT-H) elevations (Table SI-1). The plots PL-H and PL-L have been infested by insects since summers of 2004 and 2006, and all trees above the collectors died between 2004 and 2008 and 2006–2007, respectively. Afterwards, dead trunks were continuously broken by wind and only stumps of different heights remained standing in 2015. The CT-H and CT-L plots were less affected than the PL plots, and only 24% and ~6% of their vigorous trees, respectively, were broken between 2000 and 2011 (Kopáček et al., 2016). Another windthrow uprooted all trees at the CT-H plot in October 2017.

The areal densities of mature healthy trees, younger growing trees, and seedlings at all throughfall plots from 2000 to 2015 were calculated using colour aerial photographs (Table SI-1; Kopáček et al., 2016, 2017). In 2018, these numbers were based on direct counting in the field. The biomass of understory vegetation at these plots was annually estimated from 2007 to 2018 (Table SI-2).

Another two research plots were established in the PL catchment for detailed measurements of temperature and air humidity beneath living trees (LT) and in the close vicinity (~80 m) beneath dead and broken trees (DT). Both the LT and DT plots had similar elevation, slope, and aspect (Fig. SI-1). The LT forest survived the bark beetle attack due to its younger age compared to the rest of the PL catchment.

2.3. Precipitation and throughfall

Each of the bulk precipitation and throughfall plots was equipped with two and nine bulk collectors, respectively. Rain was regularly sampled at two-week intervals (May to October) using collectors protected against sample evaporation and situated 1.5–2 m above the ground. Snow was sampled at two to four-week intervals (November to April) using collectors situated 2–2.5 m above the ground. After heavy snowfall or rain, the sampling interval was shortened to avoid the loss of samples. The sampling lasted from November 1997 to December 2018 at all plots, except for the PL-H plot that was operated from November 2000. All collectors were destroyed by falling trees at the CT-H plot during a windthrow in October 2017. These collectors were replaced with 2 new ones situated in the close vicinity in an open area. After tree dieback at both PL-L and PL-H throughfall plots, sampling of precipitation continued identically to the pre-disturbance period.

Bulk precipitation and throughfall amounts were recalculated from the irregular sampling intervals to daily data (and then summed to monthly data) using daily records from the following sources: Summer daily data were from continual precipitation measurements at automatic weather stations situated at lake outlets (see next section); winter daily data were from the nearest meteorological stations, i.e. Churáňov (13.6 °E, 49.1 °N, elevation of 1118 m) and Špičácké sedlo (13.2 °E, 49.2 °N, elevation of 978 m), operated by the Czech Hydrometeorological Institute.

The annual (mm yr^{-1}) and monthly (mm $month^{-1}$) precipitation inputs (H) to the ground (forest floor and lake surface) of PL and CT catchments (H_{PL} and H_{CT}, respectively) were derived from bulk precipitation in the treeless area (H_{BP}) and throughfall (H_{TF}) at the low and high elevation plots ($H_{TF\text{-}L}$ and $H_{TF\text{-}H}$–, respectively). For more details see Kopáček et al. (2016, 2017). The monthly H_{BP}, $H_{TF\text{-}L}$ and $H_{TF\text{-}H}$ values were used to calculate $H_{TF\text{-}L}$:H_{BP}, $H_{TF\text{-}H}$:H_{BP}, and $H_{TF\text{-}H}$:$H_{TF\text{-}L}$ ratios to evaluate changes in water inputs to soil after tree dieback at the PL-L and PL-H plots.

2.4. Discharge

Discharge from the PL and CT lakes (Q_{PL} and Q_{CT}) was continuously monitored using a gauge-recorder (part of an MS4016-G automatic weather station; Fiedler AMS, České Budějovice; readings at 15-min intervals) at a weir situated close to the lake outlet (Fig. SI-1) during the 2000–2018 hydrological years (from 1 November to 31 October). Daily average discharges (m^3 day^{-1}) were summed to provide monthly (m^3 $month^{-1}$) and annual (m^3 yr^{-1}) discharges. After converting the annual discharges to mm yr^{-1}, the ratios of Q_{PL}:H_{PL} and Q_{CT}:H_{CT} were used to compare water outputs from catchments relative to the water inputs from 2002 to 2018, i.e., prior to and after the bark beetle outbreak in the PL catchment. Monthly ratios of Q_{CT}:Q_{PL} (both expressed in mm yr^{-1}) were used to determine relative changes between water outputs from the control CT and disturbed PL catchments. The years 2000 and 2001 were not included because the Q_{PL} values were affected by artificial manipulations with water level in PL Lake during this period.

2.5. Air temperature and humidity and soil temperature and moisture

Air and soil temperatures were measured at the PL-L, PL-H, LT, DT, CT-L and CT-H plots in different time intervals (Table SI-1), using TBI32–20 + 50 registration thermometers with an accuracy of ±0.4 °C, and UTBI-001 sensors with an accuracy of ±0.2 °C (Onset Computers, USA). U23-001 sensors (Onset Computers, USA) with an accuracy of ±0.2 °C and ±2.5% were used for measurements of air temperature and relative air humidity at 2 m above ground from October 2008 to December 2018. Prior to use, the thermometers were kept several days at 4 °C and then at a laboratory temperature of ~20 °C, and only thermometers that met the accuracy range of ±0.2 °C at both temperatures were used. This means that the maximum systematic difference between individual thermometers was ≤0.4 °C. Moreover, the thermometers were distributed randomly and changed in 1–3-year intervals. Hence, we can exclude that any trend herein reported was permanently affected by between-sensor differences. The thermometers were situated in solar radiation shields (diameter of 10 cm, height of 15 cm) fixed on the northern sides of wooden poles (or dead trees) 2 m above ground in the middle of the experimental plots (Fig. SI-3). Other thermometers were installed in soil at a depth of 5 cm, i.e., mostly in or just below the surface organic (litter) horizon in areas without understory vegetation and seedlings and in the close vicinity of the air thermometers at each plot. In this study, we used hourly minimum and maximum values and daily averages (arithmetical means of all 24 daily records) of soil and air temperatures.

At the LT and DT plots, eight other thermometers were situated to determine the variability in above ground air temperature (at 30 cm height) caused by topographical shading, which generally has important effects on the energy balance in complex terrains (Bellasio et al., 2005). One of the thermometers was on the same trunk as that at 2 m height in a flat area without understory vegetation, the other seven thermometers were situated on tripods in the close vicinity to cover the variability between microhabitats differing in terrain and understory characteristics (in a group of dense young spruces, in a small natural depression between rocks, below broken trunks, and in blueberry, fern, rowan and raspberry bushes; Fig. SI-3). The temperatures were recorded in 15-min intervals, and herein we use time series of daily means (arithmetic means of all 96 records per day) and daily minima and maxima.

To determine differences in soil and air temperature at the PL-L, PL-H, CT-L, and CT-H plots prior to and after tree dieback in the PL catchment, we evaluated time series of daily mean, minimum and maximum temperatures, and computed daily temperature amplitudes (the difference between maximum and minimum) for the periods 2004–2005 and 2009–2017; the year 2018 was omitted due to forest disturbance at the CT-H plot. These data were evaluated both for the whole year and growing season, defined uniformly for the purpose of this study from 1 April

to 31 October at all plots. Between-catchment differences in air temperatures were calculated for plots of similar elevations, i.e. PL-L minus CT-L and PL-H minus CT-H values. Data on air humidity were only available and evaluated for the 2009–2017 period.

The difference between soil and air temperatures and relative air humidity at plots with dead and living trees in the PL catchment were evaluated as differences between these characteristics for the DT and LT plots (DT minus LT). In addition, we evaluated variability in aboveground temperatures at 8 microhabitats within each of the DT and LT plots.

The long-term trend in air temperature reconstructed for the undisturbed CT-L plot came from Turek et al. (2014) and was updated till 2018 using the same approach (details are in Part SI-2). Data on cloudiness in the Bohemian Forest were provided by the Czech Hydrometeorological Institute, and averaged 68% during the last two decades.

Gravimetric soil moisture contents were determined as loss on drying at 105 °C at 6-week intervals at the PL-L and CT-L plots from October 2007 to December 2018. Soils were sampled from the surface organic (litter) horizon (O) and the uppermost organic rich horizon (A) during each sampling as described by Kaňa et al. (2013). In short: Samples were taken separately for each horizon from six pits (15 × 15 cm, 10–20 cm deep) and weighed. During each sampling, we prepared mixed samples for each soil horizon by combining samples from two randomly selected pits. Thus, the analyses were performed in three mixed samples of the O and A horizons. Average soil moisture was computed for each sampling period as mass weighted means for O- and A-horizons from all replicates and is relevant to the upper ~15 cm (Kopáček et al., 2018).

2.6. Statistical methods

We used the non-parametric Mann-Whitney-*U* test in XLSTAT 2019 with a significance level of 0.05 to test for differences in precipitation and throughfall amounts, soil and air temperatures, soil moisture, and air humidity between (1) the PL and CT catchments, (2) low and high elevation plots, (3) periods prior to (2004–2005) and after (2009–2017) tree dieback in the PL catchment, and (4) the DT and LT plots in the PL catchment. The null hypothesis was that the sample mean ranks were equal. A non-parametric procedure was selected because of non-normal distribution of some data (Shapiro-Wilk test). The trend analyses, including decomposing time series into three components (seasonality, trends, and random fluctuation) were done in the R environment for statistical computing (R Core Team, 2019), using the function "decompose()". The non-parametric Mann-Kendall test (Pohlert, 2018) was used to detect monotonic trends. The magnitudes of trends were computed by Sen's slope test. The function "na.seadec" from the package "imputeTS" (Moritz and Bartz-Beielstein, 2017) was used to replace missing values (November 2007 through April 2008) in time series of soil temperatures.

3. Results

3.1. Precipitation and throughfall

The annual average precipitation and throughfall amounts varied from 780 to 1981 and 815–2104 mm yr^{-1}, respectively, in both study catchments during the 1998–2018 hydrological years (Fig. 1). Throughfall amounts were significantly higher ($p < 0.001$) at the high than low elevation plots, with an 1998–2017 average $H_{TF\text{-}H}$:$H_{TF\text{-}L}$ ratio of 1.34 and throughfall gradient of 1.35 mm m^{-1} in the CT catchment. This throughfall gradient was similar to the average precipitation gradient of 1.3 mm m^{-1} in the south-western part of the Czech Republic at elevations from 900 to 1300 m (Kopáček et al., 2012). In the PL catchment, the $H_{TF\text{-}H}$:$H_{TF\text{-}L}$ ratio was similar (1.39 mm m^{-1}) to the CT catchment prior to tree dieback from 2001 to 2004. After tree dieback, however, the difference between water inputs to soils at the PL-L and PL-H plots almost disappeared (Fig. 1A), and the $H_{TF\text{-}H}$:$H_{TF\text{-}L}$ ratio significantly ($p < 0.001$) decreased to ~1.1 from 2009 to 2018 (Fig. 2A). Significant ($p < 0.001$) changes also occurred in the $H_{TF\text{-}L}$:H_{BP} and $H_{TF\text{-}H}$:H_{BP} ratios. The $H_{TF\text{-}L}$:H_{BP} ratio increased from 0.78 to 0.98 (Fig. 2B), while the $H_{TF\text{-}H}$:H_{BP} ratio decreased from 1.19 to 1.02 (Fig. 2B) in the PL catchment after the tree dieback. The $H_{TF\text{-}L}$ values were 9% lower at the PL-L than CT-L plot (average for 1998–2006), despite being 65 m higher in elevation. The $H_{TF\text{-}L}$ values, however, became almost identical ($p > 0.05$) at the PL-L and CT-L plots after tree dieback (Fig. 3A). The opposite situation occurred at high elevation plots. While the $H_{TF\text{-}H}$ values were 5% higher at the PL-H than CT-H plot from 2001 to 2004, they become 25% lower (average from 2009 to 2017) after tree dieback (Fig. 1). The changes in $H_{TF\text{-}H}$:$H_{TF\text{-}L}$:H_{BP} ratios in the PL catchment, as well as changes in throughfall ratios between the PL and CT plots, clearly show that the water amount entering soils increased at the PL-L plot, but decreased at the PL-H plot after tree dieback. A similar decrease in $H_{TF\text{-}H}$ also occurred at the CT-H plot in the 2018 hydrological year, following the plot disturbance by the windthrow (Fig. 1). In contrast, no significant between-catchment difference ($p > 0.05$) occurred for annual precipitation amounts, with average (± standard deviation) H_{BP} values of 1309 ± 225 and 1291 ± 267 mm yr^{-1} in the PL and CT catchments, respectively, during the 1998–2018 hydrological years.

3.2. Soil moisture

Despite similar water inputs to the forest floor at the PL-L and CT-L plots ($p > 0.05$) throughout 2008–2018 (Fig. 3A), soil moisture contents began to differ between the PL-L and CT-L plots soon after tree dieback (Fig. 3B). Soil moisture contents were similar (76 ± 3%; $p > 0.05$) at both plots after tree dieback until autumn 2009, but became consistently higher ($p < 0.001$) at the disturbed than control CT-L plot from 2010 to 2016, with averages of 78 vs. 73%. The difference was especially apparent (up to 17%) in the summer months of 2013 and 2015 after periods with low water inputs to soils. The between-catchment difference disappeared ($p > 0.05$) from 2017 to 2018; however, soil moisture was higher at the PL-L than CT-L plot during the very dry summer of 2018 (Fig. 3B).

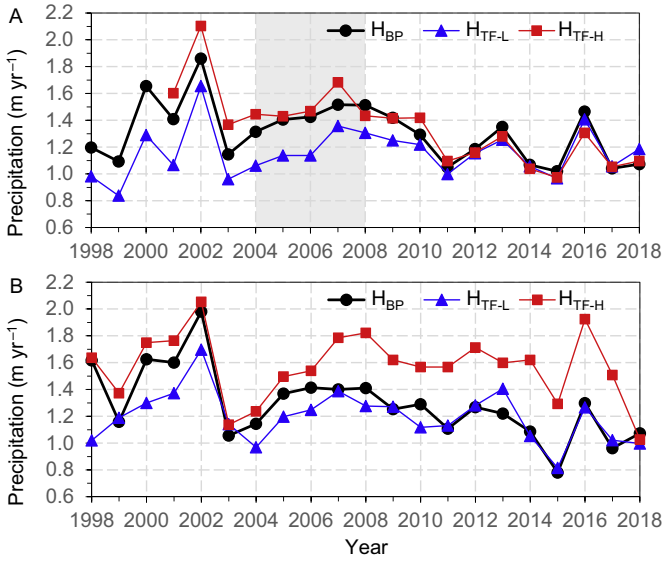

Fig. 1. Annual amounts of bulk precipitation in treeless area (H_{BP}) and throughfall at low ($H_{TF\text{-}L}$) and high ($H_{TF\text{-}H}$)– elevation plots in the Plešné (A) and Čertovo (B) catchments during the 1998–2018 hydrological years. For plot locations see Fig. SI-1. The grey area indicates the period of tree dieback in the Plešné catchment.

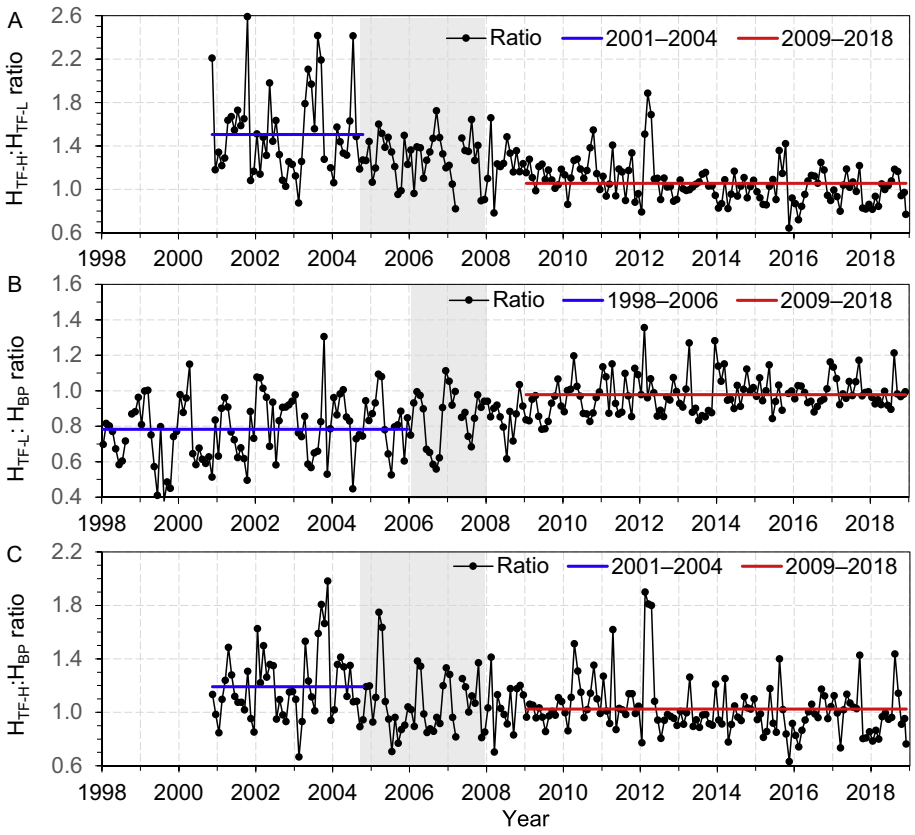

Fig. 2. Ratios among monthly values of bulk precipitation in treeless area (H_{BP}) and throughfall at low (H_{TF-L}) and high (H_{TF-H})– elevation plots in the Plešné (PL) catchment. For plot locations see Fig. SI-1. Solid lines show average H_{FT-H}:H_{TF-L} (A), H_{TF-L}:H_{BP} (B), and H_{FT-H}:H_{BP} (C) ratios prior to and after tree dieback that significantly ($p < 0.001$) differ. Grey areas indicate the period of tree dieback at the PL-L and PL-H plots.

3.3. Water balance

The respective total water inputs to the PL and CT catchments (by precipitation in treeless areas including the lake, and throughfall to the forest soil) averaged 1289 ± 203 and 1396 ± 232 mm yr^{-1}, and water outputs from lakes averaged 1118 ± 285 and 1208 ± 243 mm yr^{-1} (i.e., ~36 and ~39 L km^{-2} s^{-1}) from 2000 to 2018 hydrological years. The monthly Q_{CT}:Q_{PL} ratio averaged 1.41 from 2002 to 2005, i.e. during the period of a healthy status for most stands in both catchments (Fig. 4A). After tree dieback, this ratio decreased to 1.32, indicating a ~6% elevated discharge from the PL relative to the CT catchment (i.e., by ~70 mm yr^{-1} on average). The monthly Q_{CT}:Q_{PL} ratios varied within similar ranges prior to and after tree dieback (Fig. 4A).

The catchment annual water output to input ratios averaged 0.78 ± 0.10 for Q_{PL}:H_{PL} and 0.89 ± 0.07 for Q_{CT}:H_{CT} from 2002 to 2005 (Fig. 4B). This between-catchment difference almost disappeared immediately after tree dieback, when the Q_{PL}:H_{PL} ratio increased. Afterwards, the Q:H ratios slowly decreased in both catchments to 0.84 ± 0.04 from 2014 to 2017. The year 2018 is not included in this average because the Q_{CT}:H_{CT} ratio was elevated due to the decreased H_{TF-H} (Fig. 1) after the partial tree dieback in the CT catchment.

The observed changes in Q_{CT}:Q_{PL} and Q_{PL}:H_{PL} ratios indicate slightly elevated run-off from the PL catchment after tree dieback. The increased discharge from PL lake was not accompanied by any extreme events relative to CT lake.

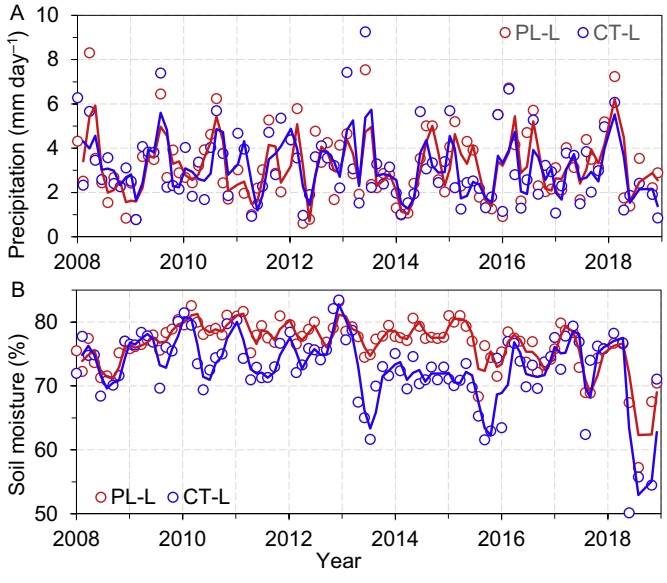

Fig. 3. Average daily throughfall to the forest floor at low elevation throughfall plots in the Plešné (PL-L) and Čertovo (CT-L) catchments during the periods between the subsequent soil samplings (A), and soil moisture at these plots (B). Solid lines are moving averages of two periods. Tree dieback occurred from 2006 to 2007 at the PL-L plot.

3.4. Between-catchment differences in air and soil temperature and air humidity

Daily mean soil and air temperatures, their minima, maxima, and daily amplitudes were expectedly higher ($p < 0.05$) at lower than higher elevation plots for almost all tested variables in both catchments (Table 1). The air temperature lapse rate (i.e., the rate at which air temperature decreases with elevation) averaged 7.4 °C km^{-1} between the PL-L and PL-H plots during both the 2004–2005 and 2009–2017 periods, while the lapse rate between the CT-L and CT-H plots was 5.5 °C km^{-1} during the identical periods. None of the tested air temperature

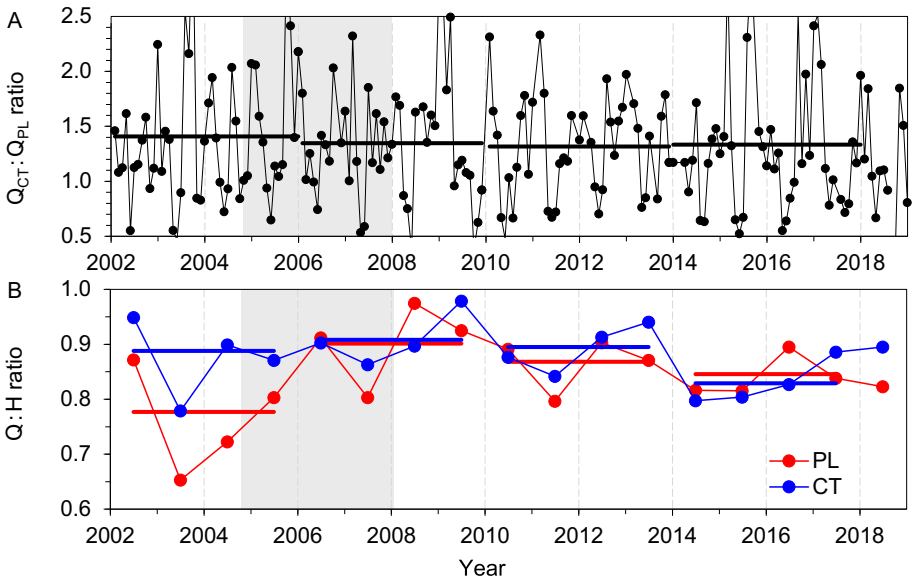

Fig. 4. Ratios between (A) monthly water discharges from Čertovo (Q_{CT}) and Plešné (Q_{PL}) lakes and (B) annual values of discharge from lakes (Q) and water input to the grounds of their respective catchments by precipitation (H). Solid lines show average Q_{CT}:Q_{PL} (A), and Q:H (B) ratios during 4-year periods from 2002 to 2017. Grey areas indicate the period of tree dieback in the PL catchment.

characteristics (except for average daily amplitude during the growing season) exhibited significant between-catchment differences from 2004 to 2005. In contrast, significant between-catchment differences occurred from 2009 to 2017 (Table 1), because air temperature increased more steeply in the PL than CT catchment even though air temperatures increased in both catchments during the study (Fig. 5A,B, Table SI-4).

In the CT catchment, air temperature increased by 1.6 and 0.5 °C on annual and growing season basis, respectively, from 2004 to 2017 (Table SI-4). The increasing temperature trends accelerated in the PL catchment after tree dieback (Fig. 5C, Table 1). Hence, the between-catchment differences in daily mean temperature increased by 0.6 °C on average after tree dieback; their average differences (PL minus CT) were −0.1 and 0.5 °C at both elevations from 2004 to 2005 and 2009–2018, respectively (Fig. 5C, Table 1). During the 2009–2018 growing seasons, daily mean air temperatures were by 1.4 and 1.2 °C higher at the PL-L and PL-H plots, respectively, than in 2004–2005, compared to the 0.5 °C increase at the CT plots (Table 1).

The greatest difference among all tested parameters occurred for maximum air temperatures, which reached values of up to 37.0 and 33.6 °C at the PL-L and PL-H plots, respectively, after tree dieback, but remained stable (~28–30 °C) at the CT plots (Table 1). The average minimum air temperatures significantly increased by 0.9–1.1 °C at all PL and CT plots between the 2004–2005 and 2009–2018 periods. A similar

Table 1
Soil temperature (0.05 m below ground) and air temperature and relative air humidity (2 m above ground) at low (L) and high (H) elevation plots in the Plešné (PL) and Čertovo (CT) catchments prior to (2004–2005) and after (2009–2017) tree dieback in the PL catchment. Symbols in superscripts indicate significant ($p < 0.05$) differences between: (a) catchments at comparable elevations, i.e. PL-L vs. CT-L and PL-H vs. CT-H in the same period; (b) low and high elevations in individual catchments, i.e. PL-L vs. PL-H and CT-L vs. CT-H in the same period; and (c) periods for individual plots, i.e. 2004–2005 vs. 2009–2017 for daily means, average minimum and maximum values, and average daily amplitude (maximum–minimum). Growing season (1 April through 31 October).

Variable	Period	Plot	Minimum in the period	Maximum in the period	Annual data			Growing season	
					Daily mean	Average minimum	Average maximum	Daily mean	Average amplitude
Soil temperature (°C)	2004–2005	PL-L	0.3	18.0	$5.4^{a,b,c}$	$5.1^{a,b,c}$	$5.8^{a,b,c}$	$8.3^{b,c}$	1.2^{c}
	2004–2005	CT-L	−1.7	23.3	$5.5^{a,b,c}$	$5.0^{a,b}$	$6.0^{a,b,c}$	$8.1^{b,c}$	$1.6^{b,c}$
	2004–2005	PL-H	−0.1	19.0	$4.5^{a,b,c}$	$4.1^{a,b,c}$	$4.9^{a,b,c}$	$6.9^{b,c}$	$1.3^{a,c}$
	2004–2005	CT-H	−2.0	21.1	$4.6^{a,b,c}$	$4.2^{a,b,c}$	$5.1^{a,b,c}$	$6.6^{b,c}$	$1.5^{a,b,c}$
	2009–2017	PL-L	−0.1	28.2	6.7^{c}	$5.7^{b,c}$	$8.0^{a,b,c}$	$10.2^{a,b,c}$	$3.7^{a,b,c}$
	2009–2017	CT-L	0.1	20.6	$5.9^{b,c}$	5.3^{b}	$6.5^{a,b,c}$	$9.0^{a,b,c}$	$2.0^{a,b,c}$
	2009–2017	PL-H	0.1	19.1	5.5^{c}	$4.9^{a,b,c}$	$6.0^{a,b,c}$	$8.5^{a,b,c}$	$1.8^{a,b,c}$
	2009–2017	CT-H	−3.1	19.5	$4.8^{b,c}$	$4.3^{a,b,c}$	$5.5^{a,b,c}$	$7.5^{a,b,c}$	$1.9^{a,b,c}$
Air temperature (°C)	2004–2005	PL-L	−15.1	28.3	$4.7^{b,c}$	$2.3^{b,c}$	$7.1^{b,c}$	$9.8^{b,c}$	$5.5^{b,c}$
	2004–2005	CT-L	−16.3	29.5	$4.8^{b,c}$	$2.4^{b,c}$	$7.3^{b,c}$	$10.0^{b,c}$	5.8
	2004–2005	PL-H	−18.0	28.9	$3.2^{b,c}$	$0.6^{b,c}$	$6.1^{b,c}$	$8.3^{b,c}$	$6.4^{a,b,c}$
	2004–2005	CT-H	−16.9	28.8	$3.3^{b,c}$	$1.0^{b,c}$	$6.0^{b,c}$	$8.4^{b,c}$	5.9^{a}
	2009–2017	PL-L	−21.3	37.0	$6.2^{a,b,c}$	$3.3^{b,c}$	$9.6^{a,b,c}$	$11.2^{a,b,c}$	$7.4^{a,b,c}$
	2009–2017	CT-L	−20.0	29.5	$5.7^{a,b,c}$	$3.3^{b,c}$	$8.4^{a,b,c}$	$10.5^{a,b,c}$	$6.1^{a,b}$
	2009–2017	PL-H	−23.9	33.6	$4.7^{a,b,c}$	$1.7^{b,c}$	$8.3^{a,b,c}$	$9.5^{a,b,c}$	$7.7^{a,b,c}$
	2009–2017	CT-H	−22.2	27.8	$4.2^{a,b,c}$	$2.1^{b,c}$	$6.9^{a,b,c}$	$8.9^{a,b,c}$	$5.6^{a,b}$
Relative air humidity (%)	2009–2017	PL-L	12	100	$81^{a,b}$	$67^{a,b}$	$92^{a,b}$	$79^{a,b}$	$28^{a,b}$
	2009–2017	CT-L	17	100	$84^{a,b}$	$74^{a,b}$	$91^{a,b}$	$81^{a,b}$	$21^{a,b}$
	2009–2017	PL-H	12	100	$84^{a,b}$	$71^{a,b}$	$94^{a,b}$	$83^{a,b}$	$27^{a,b}$
	2009–2017	CT-H	14	100	$86^{a,b}$	$77^{a,b}$	$93^{a,b}$	$85^{a,b}$	$19^{a,b}$

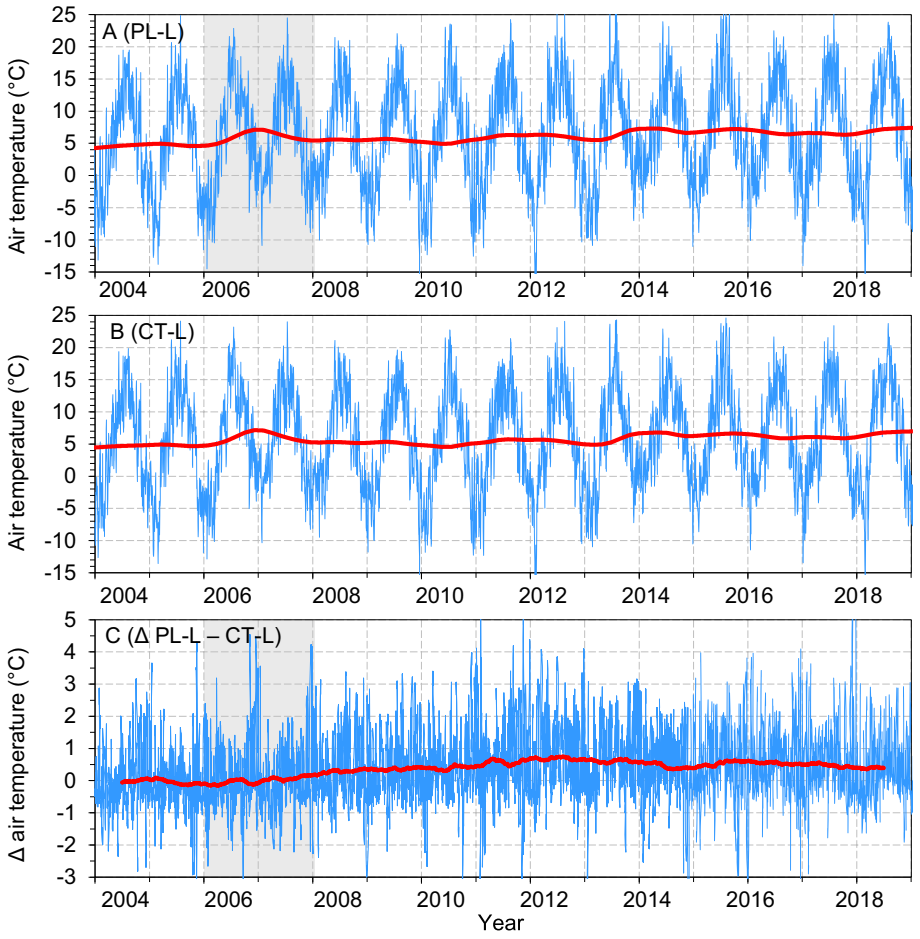

Fig. 5. Daily mean air temperature (2 m above ground) at low (L) elevation plots in the (A) Plešné (PL) and (B) Čertovo (CT) catchments, and (C) their difference (Δ PL-L – CT-L). Grey areas indicate the period of tree dieback at the PL-L plot. Solid lines: underlying trend of the metrics. All trends are significantly ($p < 0.001$) increasing, with Sen's slopes of $3.32 \cdot 10^{-4}$ (A), $2.15 \cdot 10^{-4}$ (B), and $1.27 \cdot 10^{-4}$ (C) °C d^{-1}. For details on trend analyses see Fig. SI-4.

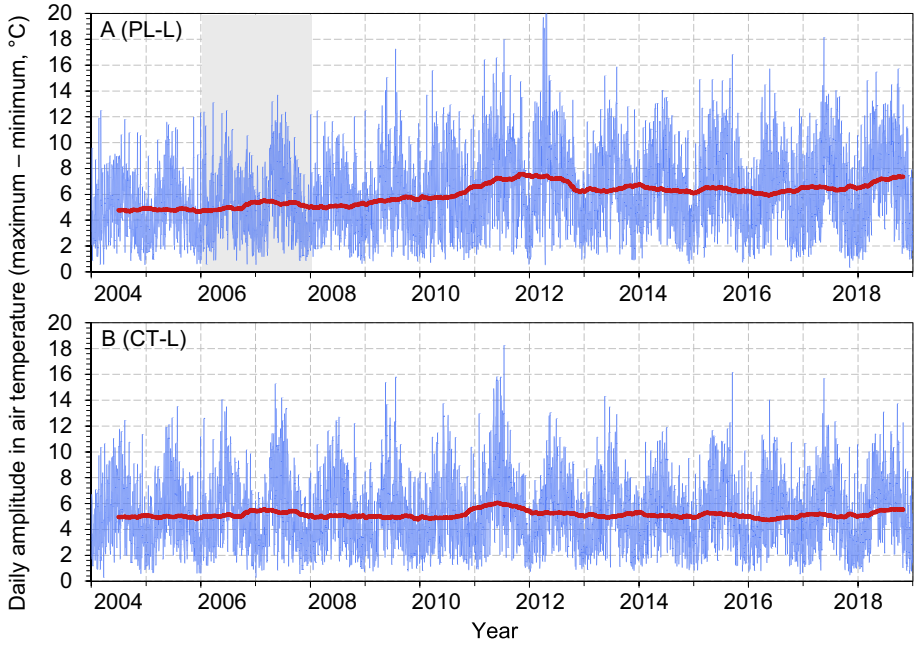

Fig. 6. Daily amplitude in air temperature (the difference between maximum and minimum) at 2 m above ground at low (L) elevation plots in the (A) Plešné (PL) and (B) Čertovo (CT) catchments. The grey area indicates the period of tree dieback at the PL-L plot. Solid lines: underlying trend of the metrics. The trend is significantly ($p < 0.001$) increasing at the PL-L plot, with Sen's slopes of $3.9 \cdot 10^{-4}$ °C d^{-1}, while the amplitude exhibits no trend ($p > 0.05$) at the CT-L plot.

increase also occurred for the average maximum air temperatures at both CT plots. In contrast, the average maximum air temperatures increased by 2.2–2.5 °C at the PL plots after tree dieback. As a result, daily amplitudes of air temperature increased in the PL catchment while remained stable at the CT plots (Fig. 6, Table SI-4). During the growing season, the post-disturbance daily temperature amplitudes increased by 2.2 and 1.3 °C on average at the PL-L and PL-H plots, respectively, while remaining stable in the control CT catchment (Table 1).

Daily mean soil temperatures were similar in both catchments, with growing season averages of ~8.3 and ~6.9 °C at the low and high elevation plots, respectively, prior to tree dieback. Daily mean soil temperatures significantly increased at all PL and CT plots from 2004 to 2017 (Table SI-4). Similarly, their minima, maxima and daily amplitudes significantly increased at all plots between the 2004–2005 and 2009–2017 periods (Table 1). The increase was, however, steeper at the disturbed PL than control CT plots (Fig. 7, Table SI-4). For daily means during growing seasons, this increase in soil temperature averaged 0.9 °C at both CT plots, while 1.9 and 1.6 °C at the PL-L and PL-H plots, respectively. As in the case of air temperature, the increases in soil temperature were more pronounced for maximum than minimum values. The minimum values of soil temperatures fell below freezing only for 5, 13, 44, and 29 days at the PL-L, CT-L, PL-H and CT-H plots, respectively, from 2004 to 2018. Most of these events occurred in late October–November, when frosts untypically occurred prior to the first snowfall. Otherwise, even a relatively thin snow cover of a few cm effectively insulated the soil from freezing at the study plots.

Relative air humidity varied in a wide range from 12 to 100% between 2009 and 2017, with minimum values during days below freezing and daily mean values averaging 79–85% during growing seasons. All tested characteristics of air humidity were significantly lower at low than at high elevation plots and at the PL than CT plots (Table 1). The average daily amplitude in air humidity was 7% lower beneath living trees at the CT plot than at the disturbed PL plots during growing seasons. The between-catchment differences most probably resulted from the absence of mature trees in the PL catchment during the measurements, as in the case of differences in air humidity between the DT and LT plots (see the next section). The trend analysis showed increasing relative air humidity at both PL plots, while no change (or even a significant decrease) occurred at the CT plots (Table SI-4).

3.5. Between-plot differences in air and soil temperature and air humidity in the Plešné catchment

The daily mean soil and air temperatures, their maxima, and daily amplitudes were significantly lower beneath the living than dead and broken trees (Table 2). The most pronounced differences occurred for above-ground air temperature (at the 0.3 m height), especially during growing seasons (Table 2). Spatial variability in minimum and maximum values of above-ground air temperature at 8 microhabitats differing in topographical and understory conditions was higher in the DT than LT plot (Fig. 8). Daily mean and maximum air temperatures were on average 0.7 and 3.5 °C higher at the DT than LT plot, respectively, during growing seasons (Table 3). At the same time, minimum values were on average 0.5 °C lower at the DT plot. Consequently, the daily amplitude in above-ground temperature was on average 4.0 °C higher at the disturbed plot than beneath leaving trees. This amplitude varied in wide ranges due to terrain and understory characteristics, with growing season averages from 5.7–12.3 °C at the DT plot and 4.8–7.2 °C at the LT plot (Table 3). For details on morphological and temperature characteristics of individual microhabitats within the DT and LT plots see Table SI-5.

The differences between maximum above-ground air temperatures observed daily for all 8 microhabitats at the DT plot vs. those observed at the LT plots were on average 5.0 °C during growing seasons (Fig. 9A). The similarly computed between-plot differences for minimum air temperatures observed at these plots were −0.6 °C during growing seasons. The opposite situation (higher minimum air temperatures at the DT than LT plots) occurred as an artefact during winter months (Fig. 9A), when higher snow cover at the DT plot than beneath living trees insulated the above-ground DT thermometers.

The between-plot differences in air temperature were on average ~50% lower at 2 m than at 0.3 m for maximum values, with daily means being on average 0.8 °C higher at the disturbed plot, and negligible differences occurring for minimum values (Fig. 9B). The differences

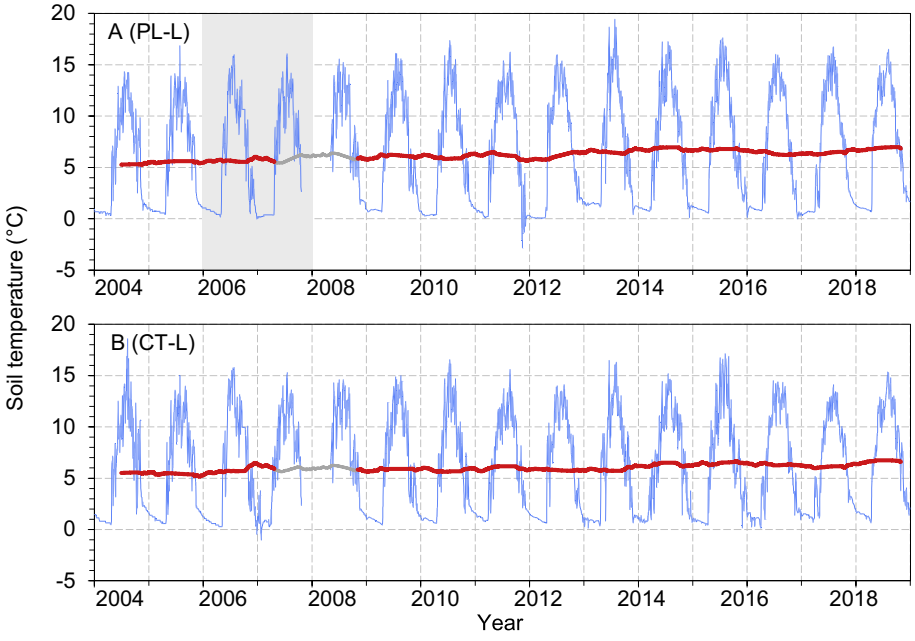

Fig. 7. Daily mean soil temperature (5 cm below ground) at low (L) elevation plots in the (A) Plešné (PL) and (B) Čertovo (CT) catchments. The grey area indicates the period of tree dieback at the PL-L plot. Solid lines: underlying trend of the metrics. Both trends are significantly ($p < 0.001$) increasing, with Sen's slopes of $9.8 \cdot 10^{-5}$ (A), and $8.6 \cdot 10^{-5}$ (B) °C d^{-1}. Grey parts of trendlines: missing values that were replaced according to Moritz and Bartz-Beielstein (2017).

Table 2
Soil and air temperature and relative air humidity at two neighbouring plots in the Plešné catchment with dead and broken trees (DT) and beneath living trees (LT) from 2012 to 2016. Asterisks indicate significant differences between the DT and LT plots (***, $p < 0.001$; **, $p < 0.01$; *, $p < 0.05$; and NS, not significant) for daily means, average minimum and maximum values, and average daily amplitudes (maximum–minimum). All parameters were measured at a similar site at each plot; growing season (1 April through 31 October).

Variable	Tree status	Minimum	Maximum	Annual data			Growing season	
				Daily mean	Average minimum	Average maximum	Daily mean	Average amplitude
Soil temperature at −0.05 m (°C)	DT	−1.8	21.5	6.2**	5.2***	7.5***	9.6*	3.4***
	LT	−1.6	18.4	5.6	5.0	6.1	8.9	1.6
Air temperature at 0.3 m (°C)	DT	−12.4	38.3	7.4***	3.9NS	12.8***	11.4***	11.1***
	LT	−13.2	29.1	6.3	3.8	9.2	10.2	6.4
Air temperature at 2 m (°C)	DT	−13.7	32.5	7.3*	3.9NS	11.6***	11.5**	8.8***
	LT	−13.4	30.0	6.7	3.9	9.7	10.7	6.6
Relative air humidity at 2 m (%)	DT	5	100	83***	68***	94***	80***	29***
	LT	8	100	86	73	95	84	24

between daily mean soil temperatures and their amplitudes at the DT and LT plots were relatively small (9.6 vs. 8.9 °C and 3.4 vs. 1.6 °C, respectively, during growing seasons; Table 2). Soil temperatures beneath living trees in the PL catchment were thus similar to those at the CT-L plot (of similar elevation) during 2009–2017 (Table 1).

Relative air humidity was significantly higher (84 vs. 80% on average) and exhibited lower daily amplitude (24 vs. 29% on average) beneath living trees than at the disturbed plot during growing seasons (Table 2). These differences were thus similar to those observed between the disturbed PL and control CT plots (Table 1).

4. Discussion

4.1. Water fluxes, soil moisture and air humidity

Tree dieback significantly affected water inputs to soils (Figs. 1 and 2). After the bark beetle outbreak, spruce rapidly lost needles within a year, and fine twigs and small branches during the following ~5 years (Kopáček et al., 2015), which continuously reduced the specific surface area of canopies. This reduction resulted in decreasing occult deposition (i.e., the sedimentation and impaction of water droplets from wind driven low clouds, mist and fog, and formation of rime and hoar frost on foliage) that importantly contributes to throughfall in central European mountain forest areas at elevations above 800 m (Eliáš et al., 1995; Tesař et al., 2000), and progressively increases with elevation (Moldan, 1991). In contrast, the decreasing surface area of canopies also reduces water evaporation (apart from transpiration) from vegetation surfaces (Beudert et al., 2007; Anderegg et al., 2012; Wehner and Stednick, 2017). Prior to tree dieback, throughfall to precipitation ratios were >1 at the PL-H plot situated at an elevation of 1334 m, while <1 at the PL-L plot (elevation of 1122 m) (Fig. 2). The smaller $H_{TF\text{-}L}$:H_{BP} ratio at the PL-L plot resulted from lower occult deposition and higher evaporation from canopies, due to the 1.5 °C higher air temperature (Table 1), than at the PL-H plot. After canopy loss, the effects of occult deposition and evaporation from tree surfaces almost ceased, and the water input to soils decreased at the high elevation plot, but increased at the low elevation plot, and they both became similar to bulk precipitation (Fig. 1). This suggests that the loss of canopies may (besides ceased transpiration) contribute to elevated run-off from disturbed forests, as generally reported in numerous studies (e.g., Beudert et al., 2007, 2018; Anderegg et al., 2012; Bearup et al., 2014), and that the magnitude of this effect is elevation-related. For the Bohemian Forest, the threshold below which the loss of canopy represents a net water gain for soils is between 1100 and 1300 m.

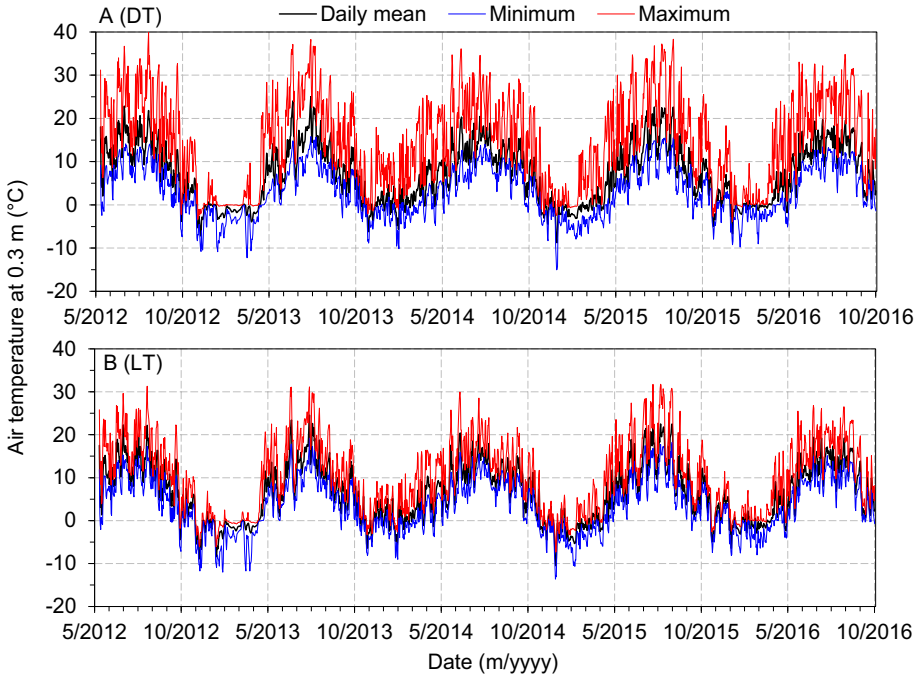

Fig. 8. Minimum, maximum and daily mean air temperatures observed above-ground (0.3 m) at 8 microhabitats with different terrain and understory characteristics beneath dead and broken (DT) and living (LT) trees in the Plešné catchment. All data are based on measurements at 15-min intervals.

Table 3
Average (± standard deviation) characteristics of air temperature (°C for all values) at 0.3 m above ground at 8 microhabitats differing in topographical and understory conditions at each of two neighbouring plots in the Plešné catchment with dead and broken trees (DT) and in the surviving forest with living trees (LT) from 2012 to 2016. Asterisks indicate significant differences between the 8 microhabitats at the DT plot vs. 8 microhabitats at the LT plot (**, $p < 0.01$; and *, $p < 0.05$) for daily means, average minimum and maximum values, and average daily amplitudes (maximum–minimum). Data on individual microhabitats within the DT and LT plots are in Table SI-5.

Plot	Annual data		Growing season	
	DT	LT	DT	LT
Daily mean	6.9 ± 0.6*	6.4 ± 0.2	10.8 ± 0.7**	10.1 ± 0.2
Average minima	3.8 ± 0.2*	4.1 ± 0.2	6.8 ± 0.3**	7.3 ± 0.2
Average maxima	11.8 ± 1.6**	9.2 ± 0.5	17.1 ± 2.0**	13.6 ± 0.6
Average amplitude	8.0 ± 1.7**	5.1 ± 0.6	10.3 ± 2.2**	6.3 ± 0.7
Amplitude range	4.4–9.4	3.8–5.8	5.7–12.3	4.8–7.2

The interplay between occult deposition and interception also contributed to seasonal variations in throughfall to precipitation ratios, with maximum values in winter and minimum values in summer (Fig. 2). This seasonal variation resulted from the higher contribution of occult deposition to throughfall in winter, along with higher evaporation from canopies in summer (Moldan, 1991), and continuously decreased with decreasing canopy surface after tree dieback.

Besides decreased transpiration and interception, the loss of canopy cover from tree mortality increases radiation and wind at the ground surface, which both increase soil evaporation and understory transpiration (Anderegg et al., 2012). Because pre-disturbance transpiration by mature trees is usually higher than post-disturbance increases in evapotranspiration from soils and understory vegetation, the net results are elevated soil moisture and run-off from disturbed forests (Bearup et al., 2014; Caldwell et al., 2016; Beudert et al., 2018). A similar situation occurred in the disturbed PL forest, where soil moisture increased after tree dieback and remained relatively stable and higher than at the undisturbed CT forest for 5–6 subsequent years despite similar water inputs (Fig. 3). The rapidly increasing density of regenerating trees (Fig. SI-2, Table SI-2) and increasing biomass of understory vegetation at the PL-L plot (Table SI-3) resulted in increasing transpiration, and soil moisture at both localities again became similar. This increasing transpiration was the likely reason for significantly increasing air humidity at both PL plots from 2009 to 2017, while a slight decrease or no change in air humidity occurred at the CT plots (Table SI-4). The effect of the ceased transpiration of dead mature trees on differences in relative air humidity between the living and dead stands (Tables 1 and 2) thus started to diminish about one decade after tree dieback at the PL-L and PL-H plots.

The rapid tree re-growth in the PL catchment shows that mountain spruce forests are restored through advance regeneration (Messier et al., 1999), with the majority of seedlings established before the disturbance (Bače et al., 2015; Macek et al., 2017). Bark beetle disturbances harm these seedlings and their natural environment significantly less than salvage logging, which disturbs the vegetation cover and reduces advance regeneration densities (Nováková and Edwards-Jonášová, 2015; Michalová et al., 2017), and/or less than windthrows and tree uprooting, which create pit and mound topography with bare mineral soil (Vodde et al., 2010; Michalová et al., 2017). Stands regenerating after bark beetle attacks in unmanaged areas have a heterogeneous structure due to the predominant association of seedlings with specific microhabitats, like dead wood (Bače et al., 2015). A post-disturbance rapid growth of seedlings is enabled by enhanced light conditions (Messier et al., 1999; Bače et al., 2015). Moreover, the survival of these seedlings is more successful at unmanaged sites than in clear-cut and artificially reforested areas (Nováková and Edwards-Jonášová, 2015; Zeppenfeld et al., 2015) due to the protecting effect of dead trees (Macek et al., 2017), higher nutrient availability in soils from decomposing dead biomass (Kaňa et al., 2013, 2019; Tahovská et al., 2018), and stable and available soil moisture (Fig. 3B).

A wide range in the response of hydrology to forest disturbances and regrowth has been reported, from negligible effects compared to those related to changes in climate and snowmelt timing (Slinski et al., 2016) to large changes in run-off (Caldwell et al., 2016). Our results suggest a relatively modest (~6%) increase in run-off from the disturbed PL catchment after bark-beetle induced tree mortality (Fig. 4). This small increase was similar to those observed in nearby larger catchments (Upper Große Ohe and Forellenbach) in the Bavarian Forest, after 40–60% of forest area was disturbed by a bark beetle infestation

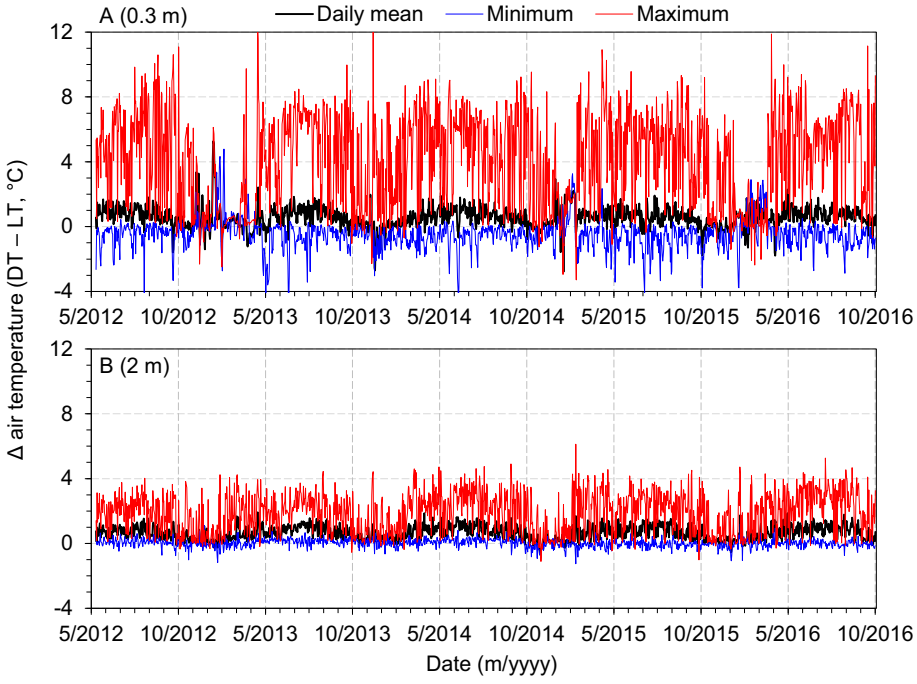

Fig. 9. Between-plot differences in daily mean, minimum and maximum air temperatures beneath dead and broken (DT) and living (LT) trees in the Plešné catchment at (A) 0.3 m (the difference between values given in Fig. 8A and B) and (B) 2 m above ground. All data are based on measurements at 15-min intervals.

(Beudert et al., 2018). The Q_{CT}:Q_{PL} ratios varied within similar ranges prior to and after tree dieback (Fig. 4A), indicating no extreme hydrological events after the PL forest disturbance, despite the steepness of the catchment. Moreover, we observed no signs of soil erosion during repeated soil sampling throughout the PL catchment in 2010 and 2015 (no landslides and/or missing uppermost soil horizons). The residence of water in PL Lake could possibly have partly mitigated elevated flows from its catchment, but negligible modifications in peak flows after forest disturbance have also been observed in other unmanaged catchments (Slinski et al., 2016; Beudert et al., 2018). This is in contrast to elevated peak flows from clear-cut areas (Caissie et al., 2002). Beudert et al. (2018) explained the difference between these extreme management practices by unaffected soils and understory vegetation and more coarse woody debris in unmanaged areas. Soil compaction and rut formation by heavy machinery leads to increasing surface flow, forced erosion, and accelerated run-off generation in managed areas (Beschta, 1978, Beudert et al., 2018).

4.2. Air and soil temperature

Air and soil temperatures significantly increased during our study at all research plots (Table SI-4), despite the extent of their disturbance due especially to the unprecedentedly highest air temperatures since 1781 that occurred from 2014 to 2018 as an effect of global warming (Fig. SI-5). All measured temperatures expectedly increased more steeply at the disturbed than control plots (Tables 1 and 3). The highest differences between the disturbed and control plots occurred for above-ground temperature, with differences ranging between 0.8 and 1.1 °C and 0.7–1.0 °C at 2 m above ground and at 5 cm below ground, respectively, during growing seasons. While the differences between daily mean air and soil temperatures at disturbed and control plots were relatively small, larger differences occurred for daily maxima and amplitudes (Figs. 8 and 9). These differences were especially high during sunny days, but their averages were less pronounced (Table 2).

The relatively small differences in daily mean air and soil temperatures between disturbed and undisturbed forests generally result from their lower values in the day and relatively warmer conditions at night beneath the living trees due to the effect of their transpiration and long-wave radiation, respectively (Chen et al., 1999; Tesař et al., 2006). Consequently, lower daily maxima and higher daily minima in forests than in open land are typical for diurnal patterns in air temperatures at paired sites located at latitudes from 28 to 45°N (Lee et al., 2011). This pattern was especially evident for microhabitats at the DT and LT plots, with the respective maxima in daily temperatures averaging from 12.9–19.0 and 12.4–14.5 °C, and minima averaging from 6.4–7.2 and 7.0–7.6 °C at 0.3 m above ground during growing seasons (Table SI-5).

The spatial variability in above-ground temperatures was higher among the DT than LT microhabitats (Table 3). The microhabitats in natural depressions or below broken trunks at the disturbed plot had similar above-ground temperatures to those above the bare litter horizon at the undisturbed plot (Table SI-5). This large variability of microclimate in forest undergrowth is one of the most important biological legacies following natural disturbances; these post-disturbance structures promote microsite diversity and associated biodiversity, including regeneration of various tree species (Swanson et al., 2011). Between-microhabitat variability is very important due to its large potential to buffer extreme climate events and thus decrease the vulnerability of ambient communities (Scheffers et al., 2014). For instance, Farská et al. (2014) observed that the impact of disturbance on soil invertebrates was mitigated by more rapid forest regeneration and more complicated microrelief (with dead wood-sheltered microhabitats) in unmanaged than clear-cut areas. Similarly, Čuchta and Shrubovych (2015) and Kokořová and Starý (2017) observed significant differences in the composition of the soil mesofauna community between naturally regenerating vs. managed spruce forests, which was more abundant in unmanaged areas, as well as more similar to the communities in undisturbed mature forests.

4.2.1. Air and soil temperature vs. surface temperature

The ranges in maximum daily above-ground temperatures observed at the DT and LT microhabitats (Fig. 9, Table SI-5) were relatively narrow compared to the wide differences in maximum surface temperatures observed in the study region during sunny days. For example, Hojdová et al. (2005) observed maximum ground surface temperatures of 28, 42, and 52 °C in an undisturbed forest, dry forest, and peat bog (*Sphagnum* moss), respectively. Similarly, Matějka (*unpublished data*) measured a range of ground temperatures varying from 23 °C at a surface shaded by grass to 60 °C at a bare surface exposed to full sunshine at the PL-H plot at noon on 23 July 2019. The maximum air and soil temperatures at 2 m above ground and at 5 cm below ground were 26.6 and 15.0 °C at the latter microhabitat, respectively (Turek, *unpublished data*), suggesting that a ground surface temperature of 60 °C cannot be used as a realistic proxy for environmental interpretations.

Even greater problems with environmental interpretations of surface temperatures occur for studies based on surface temperatures estimated by remote sensing (Hesslerová et al., 2018). Many distant data studies are based on measurements during sunny days and represent extreme rather than "average" conditions, especially for mountainous areas like the Bohemian Forest, with an average cloudiness of 68%. Moreover, these methods are biased by surface temperatures of dead trunks, which overestimate the measurements. Dead trunks also provide shade and limit wind speed, thus maintain microclimatic variability in their surroundings and underlying soils. These conditions (together with stable soil moisture) enable the more successful regeneration and survival of seedlings (Macek et al., 2017), mitigate impacts on soil invertebrates (Farská et al., 2014; Kokořová and Starý, 2017), and limit the temperature effect on soil microbial processes, like mineralization and nitrogen cycling (Šantrůčková et al., 2009). While remote sensing is useful for tracking spatial variability and relative changes in surface temperatures for vast areas (e.g., Hais and Kučera, 2009), its use in regional models (Hesslerová et al., 2018) may lead to significant misinterpretations and overestimations of the real impacts of disturbances on forest ecosystems.

5. Conclusions

We observed statistically significant, but relatively small responses in hydrology and microclimatic characteristics to tree dieback in the PL catchment (despite the 93% tree dieback, thin soils, and steep mountainous terrain), which were within ranges reported for disturbed lower elevation catchments elsewhere (e.g., Chen et al., 1999; Brown et al., 2005; Beudert et al., 2018). The disturbance-induced increases in daily mean soil and air temperatures observed during growing seasons were 0.7–1.0 °C higher in the disturbed PL catchment than their parallel increases of 0.9 and 0.5 °C, respectively, due to climate change in the control CT catchment from 2004 to 2017 (Tables 1 and 2). The effects of tree dieback in the unmanaged forest and climate change were thus of the same magnitude. Moreover, high spatial variability among microhabitats (representing different terrain and understory characteristics, Table 3) provided possible refuges for original species after the forest disturbance and limited the risk of their extinction prior to forest regeneration.

The actual effects of tree dieback after bark beetle infestation on hydrology, microclimate, and original biodiversity are thus less pronounced and more variable in unmanaged, naturally disturbed areas than in clear-cut areas (Hais and Kučera, 2008; Farská et al., 2014; Zeppenfeld et al., 2015; Beudert et al., 2018). Our data clearly suggest that the effects of natural forest disturbances in unmanaged areas on regional climate, predicted on the basis of satellite or thermovision camera images (e.g., Hesslerová et al., 2018), are not fully reliable.

CRediT authorship contribution statement

Jiří Kopáček: Conceptualization, Formal analysis, Writing - original draft, Funding acquisition.**Radek Bače:**Methodology, Investigation, Writing - original draft.**Josef Hejzlar:**Data curation, Formal analysis, Writing - original draft.**Jiří Kaňa:**Methodology, Investigation, Formal analysis, Writing - original draft.**Tomáš Kučera:**Conceptualization, Formal analysis, Writing - original draft.**Karel Matějka:**Methodology, Investigation.**Petr Porcal:**Data curation, Formal analysis, Visualization. **Jan Turek:**Investigation, Data curation, Validation, Visualization.

Declaration of competing interest

The authors declare that they have no known competing financial interests or personal relationships that could have appeared to influence the work reported in this paper.

Acknowledgments

We thank the authorities of the Šumava National Park for their administrative support and D. W. Hardekopf for proofreading. This study was supported by the Czech Science Foundation (project No. P503-19-16605S) and Czech Academy of Sciences (project StrategyAV21-Environmental Threats). The data used are listed in the references and supplements.

Appendix A. Supplementary data

Supplementary data associated with this article can be found in the online version, at https://doi.org/10.1016/j.scitotenv.2020.137518. These data include the Google map of the most important areas described in this article.

References

Aber, J.D., Driscoll, C.T., 1997. Effects of land use, climate variation, and N deposition on N cycling and C storage in northern hardwood forests. Global Biogeochem. Cy. 11 (4), 639–648.

Anderegg, W.R.L., Kane, J.M., Anderegg, L.D.L., 2012. Consequences of widespread tree mortality triggered by drought and temperature stress. Nat. Clim. Chang. 3, 30–36. https://doi.org/10.1038/NCLIMATE1635.

Bače, R., Svoboda, M., Janda, P., Morrissey, R.C., Wild, J., Clear, J.L., Čada, V., Donato, D.C., 2015. Legacy of pre-disturbance spatial pattern determines early structural diversity following severe disturbance in montane spruce forests. PLoS One 10 (9), e0139214. http://10.1371/journal.pone.0139214.

Bearup, L.A., Maxwell, R.M., Clow, D.W., McCray, J.E., 2014. Hydrological effects of forest transpiration loss in bark beetle-impacted watersheds. Nat. Clim. Chang. 4 (6), 481–486. https://doi.org/10.1038/nclimate2198.

Bellasio, R., Maffeis, G., Scire, J.S., Longoni, M.G., Bianconi, R., Quaranta, N., 2005. Algorithms to account for topographic shading effect and surface temperature dependence on terrain elevation in diagnostic meteorological models. Bound. Lay. Meteorol. 114 (3), 595–614. https://doi.org/10.1007/s10546-004-1670-6.

Beschta, R.L., 1978. Long-term patterns of sediment production following road construction and logging in the Oregon Coast Range. Water Resour. Res. 14, 1011–1016. https://doi.org/10.1029/WR014i006p01011.

Beudert, B., Klöcking, B., Schwarze, R., 2007. Grosse Ohe: impact of bark beetle infestation on the water and matter budget of a forested catchment. In: Puhlmann, H., Schwarze, R. (Eds.), Forest Hydrology – Results of Research in Germany and Russia. IHP/HWRP, Berichte 6, Koblenz, pp. 41–62.

Beudert, B., Bernsteinová, J., Premier, J., Bässler, C., 2018. Natural disturbance by bark beetle offsets climate change effects on streamflow in headwater catchments of the Bohemian Forest. Silva Gabreta 24, 21–45.

Brown, A.E., Zhang, L., McMahon, T.A., Western, A.W., Vertessy, R.A., 2005. A review of paired catchment studies for determining changes in water yield resulting from alterations in vegetation. J. Hydrol. 310, 28–61. https://doi.org/10.1016/j.jhydrol.2004.12.010.

Caissie, D., Jolicoeur, S., Bouchard, M., Poncet, E., 2002. Comparison of streamflow between pre and post timber harvesting in Catamaran Brook (Canada). J. Hydrol. 258 (1–4), 232–248. https://doi.org/10.1016/S0022-1694(01)00576-5.

Caldwell, P.V., Miniat, C.F., Elliott, K.J., Swank, W.T., Brantley, S.T., Laseter, S.H., 2016. Declining water yield from forested mountain watersheds in response to climate change and forest mesophication. Glob. Change Biol. 22, 2997–3012. https://doi.org/10.1111/gcb.13309.

Chen, J., Franklin, J.F., 1997. Growing-season microclimate variability within an old-growth Douglas-fir forest. Clim. Res. 8, 21–34.

Chen, J., Saunders, S.C., Crow, T.R., Naiman, R.J., Brosofske, K.D., Mroz, G.D., Brookshire, B.L., Franklin, J.F., 1999. Microclimate in forest ecosystem and landscape ecology: variations in local climate can be used to monitor and compare the effects of different management regimes. BioScience 49 (4), 288–297. http://www.jstor.org/stable/10.1525/bisi.1999.49.4.288.

Čuchta, P., Shrubovych, J., 2015. Soil Collembola communities in montane coniferous forests of the Bohemian Forest. Silva Gabreta 21 (2), 149-146.

Edburg, S.L., Hick, J.A., Brooks, P.D., Pendall, E.G., Ewers, B.E., Norton, U., Gochis, D.J., Gutmann, E.D., Meddens, A.J., 2012. Cascading impacts of bark beetle-caused tree mortality on coupled biogeophysical and biogeochemical processes. Front. Ecol. Environ. 10, 416–424. https://doi.org/10.1890/110173.

Ehbrecht, M., Schall, P., Ammer, C., Fischer, M., Seidel, D., 2019. Effects of structural heterogeneity on the diurnal temperature range in temperate forest ecosystems. Forest Ecol. Manag. 432, 860–867. https://doi.org/10.1016/j.foreco.2018.10.008.

Eliáš, V., Tesař, M., Buchtele, J., 1995. Occult precipitation: sampling, chemical analysis and process modelling in the Sumava Mts., (Czech Republic) and in the Taunus Mts. (Germany). J. Hydrol. 166 (3–4), 409–420. https://doi.org/10.1016/0022-1694(94)05096-G.

Farská, J., Prejzková, K., Starý, J., Rusek, J., 2014. Soil microarthropods in non-intervention montane spruce forest regenerating after bark-beetle outbreak. Ecol. Res. 29, 1087–1096. https://doi.org/10.1007/s11284-014-1197-3.

Hais, M., Kučera, T., 2008. Surface temperature change of spruce forest as a result of bark beetle attack: remote sensing and GIS approach. Eur. J. Forest Res. 127 (4), 327–336. https://doi.org/10.1007/s10342-008-0208-8.

Hais, M., Kučera, T., 2009. The influence of topography on the forest surface temperature retrieved from Landsat TM, ETM + and ASTER thermal channels. ISPRS J. Photogramm. 64, 585–591. https://doi.org/10.1016/j.isprsjprs.2009.04.003.

Hesslerová, P., Huryna, H., Pokorný, J., Procházka, J., 2018. The effect of forest disturbance on landscape temperature. Ecol. Eng. 120, 345–354. https://doi.org/10.1016/j.ecoleng.2018.06.011.

Hojdová, M., Hais, M., Pokorný, J., 2005. Microclimate of a peat bog and of the forest in different states of damage in the Šumava National Park. Silva Gabreta 11 (1), 13–24.

Houlton, B.Z., Driscoll, C.T., Fahey, T.J., Likens, G.E., Groffman, P.M., Bernhardt, E.S., Buso, D.C., 2003. Nitrogen dynamics in ice storm-damaged forest ecosystems: implications for nitrogen limitation theory. Ecosystems 6, 431–443. https://doi.org/10.1007/s10021-002-0198-1.

Kaňa, J., Tahovská, K., Kopáček, J., 2013. Response of soil chemistry to forest dieback after bark beetle infestation. Biogeochemistry 113, 369–383. https://doi.org/10.1007/s10533-012-9765-5.

Kaňa, J., Kopáček, J., Tahovská, K., Šantrůčková, H., 2019. Tree dieback and related changes in nitrogen dynamics modify the concentrations and proportions of cations on soil sorption complex. Ecol. Indic. 97, 319–328. https://doi.org/10.1016/j.ecolind.2018.10.032.

Kokořová, P., Starý, J., 2017. Communities of oribatid mites (Acari: Oribatida) of naturally regenerating and salvage-logged montane spruce forests of Šumava Mountains. Biologia 72, 445–451. https://doi.org/10.1515/biolog-2017-0050.

Kopáček, J., Posch, M., Hejzlar, J., Oulehle, F., Volková, A., 2012. An elevation-based regional model for interpolating sulphur and nitrogen deposition. Atmos. Environ. 50, 287–296. https://doi.org/10.1016/j.atmosenv.2011.12.017.

Kopáček, J., Cudlín, P., Fluksová, H., Kaňa, J., Picek, T., Šantrůčková, H., Svoboda, M., Vaňek, D., 2015. Dynamics and composition of litterfall in an unmanaged Norway spruce (*Picea abies*) forest after bark-beetle outbreak. Boreal Environ. Res. 20, 305–323.

Kopáček, J., Hejzlar, J., Kaňa, J., Porcal, P., Turek, J., 2016. The sensitivity of water chemistry to climate in a forested, nitrogen-saturated catchment recovering from acidification. Ecol. Indic. 63, 196–208. https://doi.org/10.1016/j.ecolind.2015.12.014.

Kopáček, J., Fluksová, H., Hejzlar, J., Kaňa, J., Porcal, P., Turek, J., 2017. Changes in surface water chemistry caused by natural forest dieback in an unmanaged mountain catchment. Sci. Total Environ. 584–585, 971–981. https://doi.org/10.1016/j.scitotenv.2017.01.148.

Kopáček, J., Evans, C.D., Hejzlar, J., Kaňa, J., Porcal, P., Šantrůčková, H., 2018. Factors affecting the leaching of dissolved organic carbon after tree dieback in an unmanaged European mountain forest. Environ. Sci. Technol. 52, 6291–6299. https://doi.org/10.1021/acs.est.8b00478.

Lee, X., Goulden, M.L., Hollinger, D.Y., Barr, A., Black, A.T., Gil, B., Bracho, R., Drake, B., Goldstein, A., Gu, L., Katul, G., Kolb, T., Law, B.E., Margolis, H., Meyers, T., Monson, R., Munger, W., Oren, R., Tha Paw, U,.K., Richardson, A.D., Schmid, H.P., Staebler, R., Wofsy, S., Zhao, L., 2011. Observed increase in local cooling effect of deforestation at higher latitudes. Nature 479, 384–387. https://doi.org/10.1038/nature10588.

Macek, M., Wild, J., Kopecký, M., Červenka, J., Svoboda, M., Zenáhlíková, J., Brůna, J., Mosandl, R., Fischer, A., 2017. Life and death of Picea abies after bark-beetle outbreak: ecological processes driving seedling recruitment. Ecol. Appl. 27 (1), 156–167. https://doi.org/10.1002/eap.1429.

Matějka, K., 2015. Disturbance-induced changes in the plant biomass in forests near Plešné and Čertovo Lakes. J. Forest Sci. 61 (4), 156–168. https://doi.org/10.17221/109/2014-JFS.

Messier, C., Doucet, R., Ruel, J., Claveau, Y., Kelly, C., Lechowicz, M.J., 1999. Functional ecology of advance regeneration in relation to light in boreal forests. Can. J. For. Res. 29, 812–823. https://doi.org/10.1139/x99-070.

Michalová, Z., Morrissey, R., Wohlgemuth, T., Bače, R., Fleischer, P., Svoboda, M., 2017. Salvage-logging after windstorm leads to structural and functional homogenization of understory layer and delayed spruce tree recovery in Tatra Mts., Slovakia. Forests 8 (3), 88. https://doi.org/10.3390/f8030088.

Mikkelson, K.M., Dickerson, E.R.V., Maxwell, R.M., McCray, J.E., Sharp, J.O., 2013. Water-quality impacts from climate-induced forest die-off. Nat. Clim. Chang. 3, 218–222. https://doi.org/10.1038/NCLIMATE1724.

Moldan, B., 1991. Atmospheric Deposition: A Biogeochemical Process. Academia, Prague.

Moritz, S., Bartz-Beielstein, T., 2017. The R J 9 (1), 207–218. https://doi.org/10.32614/RJ-2017-009.
Nováková, M.H., Edwards-Jonášová, M., 2015. Restoration of central-European mountain Norway spruce forest 15 years after natural and anthropogenic disturbance. Forest Ecol. Manag. 344, 120–130. https://doi.org/10.1016/j.foreco.2015.02.010.
Oulehle, F., Cosby, B.J., Wright, R.F., Hruška, J., Kopáček, J., Krám, P., Evans, C.D., Moldan, F., 2012. Modelling soil nitrogen: the MAGIC model with nitrogen retention linked to carbon turnover using decomposer dynamics. Environ. Pollut. 165, 158–166. https://doi.org/10.1016/j.envpol.2012.02.021.
Oulehle, F., Wright, R.F., Svoboda, M., Bače, R., Matějka, K., Kaňa, J., Hruška, J., Couture, R.-M., Kopáček, J., 2019. Effects of bark beetle disturbance on soil nutrient retention and lake chemistry in glacial catchment. Ecosystems 22, 725–741. https://doi.org/10.1007/s10021-018-0298-1.
Pohlert, T., 2018. Trend: non-parametric trend tests and change-point detection. R package version 1.1.1 https://CRAN.R-project.org/package=trend.
R Core Team, 2019. R: A Language and Environment for Statistical Computing. R Foundation for Statistical Computing, Vienna, Austria https://www.R-project.org/.
Šantrůčková, H., Tahovská, K., Kopáček, J., 2009. Nitrogen transformations and pools in N-saturated mountain spruce forest soils. Biol. Fert. Soils 45, 395–404. https://doi.org/10.1007/s00374-008-0349-4.
Scheffers, B.R., Edwards, D.P., Diesmos, A., Williams, S.E., Evans, T.A., 2014. Microhabitats reduce animal's exposure to climate extremes. Glob. Change Biol. 20 (2), 495–503. https://doi.org/10.1111/gcb.12439.
Seidl, R., Thom, D., Kautz, M., Martin-Benito, D., Peltoniemi, M., Vacchiano, G., Wild, J., Ascoli, D., Petr, M., Honkaniemi, J., Lexer, M.J., Trotsiuk, V., Mairota, P., Svoboda, M., Fabrika, M., Nagel, T.A., Reyer, C.P.O., 2017. Forest disturbances under climate change. Nat. Clim. Chang. 7, 395–402. https://doi.org/10.1038/nclimate3303.
Slinski, K.M., Hogue, T.S., Porte, r A.T., McCray, J.E., 2016. Recent bark beetle outbreaks have little impact on streamflow in the Western United States. Environ. Res. Lett. 11, 074010. https://doi.org/10.1088/1748-9326/11/7/074010.
Svoboda, M., Matějka, K., Kopáček, J., 2006. Biomass and element pools of understory vegetation in the catchments of Čertovo Lake and Plešné Lake in the Bohemian Forest. Biologia 61 (Suppl. 20), S509–S521. https://doi.org/10.2478/s11756-007-0074-8.
Swanson, M.E., Franklin, J.F., Beschta, R.L., Crisafulli, C.M., DellaSala, D.A., Hutto, R.L., Lindenmayer, D.B., Swanson, F.J., 2011. The forgotten stage of forest succession: early-successional ecosystems on forest sites. Front. Ecol. Environ. 9 (2), 117–125. https://doi.org/10.1890/090157.
Tahovská, K., Čapek, P., Šantrůčková, H., Kopáček, J., 2018. In situ phosphorus dynamics in soil: long-term ion-exchange resin study. Biogeochemistry 139, 307–320. https://doi.org/10.1007/s10533-018-0470-x.
Tesař, M., Fottová, D., Eliáš, V., Šír, M., 2000. Occult precipitation as an important contribution to the wet deposition in Bohemian Forest. Silva Gabreta 4, 87–96.
Tesař, M., Šír, M., Lichner, L., Zelenková, E., 2006. Influence of vegetation cover on thermal regime of mountainous catchments. Biologia 61 (Suppl. 19), S311–S314. https://doi.org/10.2478/s11756-006-0179-5.
Turek, J., Fluksová, H., Hejzlar, J., Kopáček, J., Porcal, P., 2014. Modelling air temperature in catchments of Čertovo and Plešné lakes in the Bohemian Forest back to 1781. Silva Gabreta 20, 1–24.
Vodde, F., Jogiste, K., Gruson, L., Ilisson, T., Köster, K., Stanturf, J.A., 2010. Regeneration in windthrow areas in hemiboreal forests: the influence of microsite on the height growths of different tree species. J. For. Res. 15 (1), 55–64. https://doi.org/10.1007/s10310-009-0156-2.
Wehner, C.E., Stednick, J.D., 2017. Effects of mountain pine beetle-killed forests on source water contributions to streamflow in headwater streams of the Colorado Rocky Mountains. Front. Earth Sci. 11 (3), 496–504. https://doi.org/10.1007/s11707-017-0660-1.
Wei, X., Zhang, M., 2010. Quantifying streamflow change caused by forest disturbance at a large spatial scale: a single watershed study. Water Resour. Res. 46, W12525. https://doi.org/10.1029/2010WR009250.
Zeppenfeld, T., Svoboda, M., DeRose, R.J., Heurich, M., Müller, J., Čížková, P., Starý, M., Bače, R., Donato, D.C., 2015. Response of mountain *Picea abies* forests to stand-replacing bark beetle outbreaks: neighbourhood effects lead to self-replacement. J. Appl. Ecol. 52 (5), 1402–1411. https://doi.org/10.1111/1365-2664.12504.

Supplementary Information to

Changes in microclimate and hydrology in an unmanaged mountain forest catchment after insect-induced tree dieback

Jiří Kopáček[1,2], Radek Bače[3], Josef Hejzlar[1], Jiří Kaňa[1,2], Tomáš Kučera[2], Karel Matějka[4], Petr Porcal[1,2], Jan Turek[1]

[1]Biology Centre of the Czech Academy of Sciences, Institute of Hydrobiology, České Budějovice, Czech Republic,
[2]University of South Bohemia, Faculty of Science, České Budějovice, Czech Republic,
[3]Czech University of Life Sciences, Faculty of Forestry and Wood science, Prague, Czech Republic
[4]IDS, Prague, Czech Republic

(Supplementary Information includes 9 pages, 5 figures, and 5 tables)

Part SI-1: Details to Materials and Methods

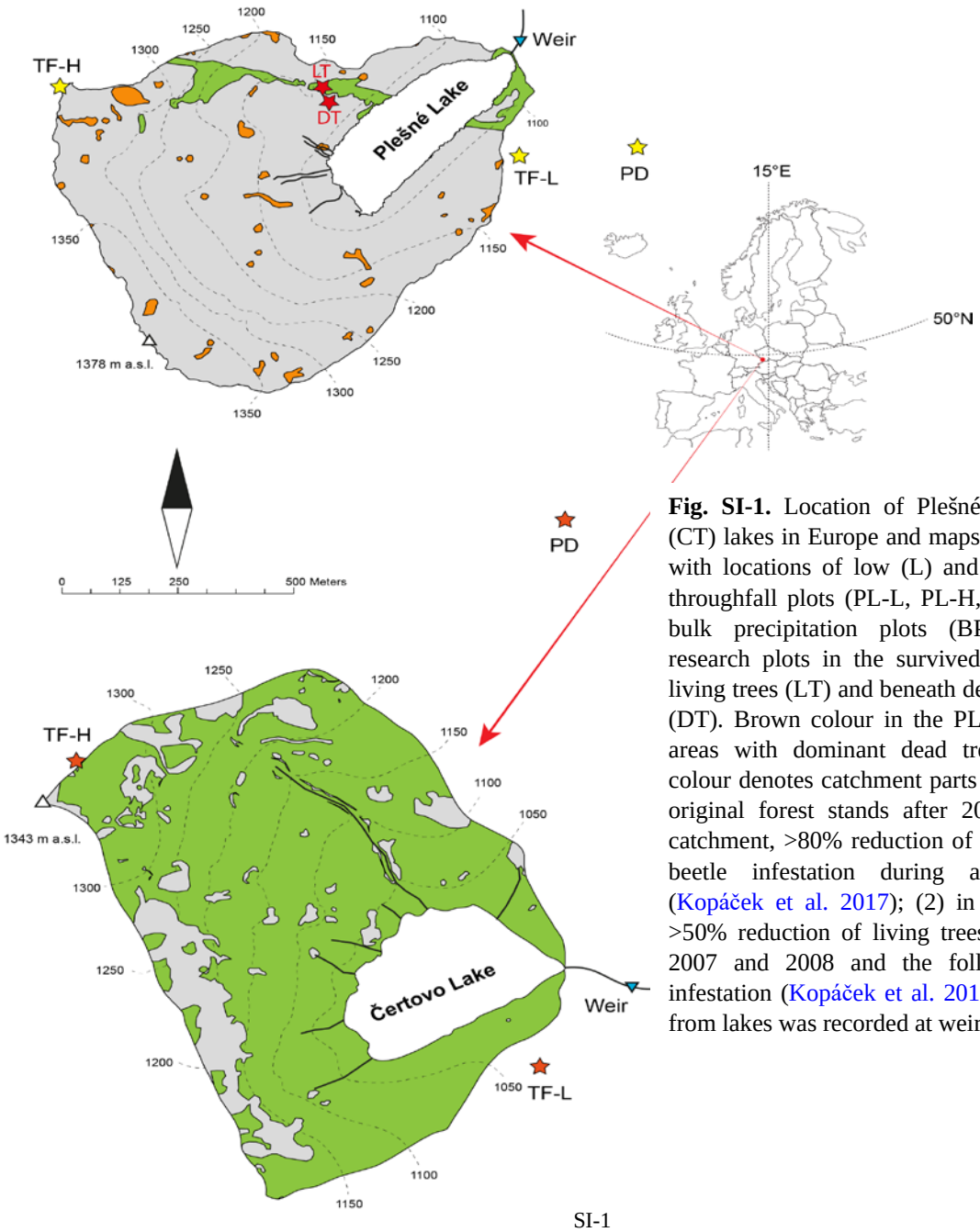

Fig. SI-1. Location of Plešné (PL) and Čertovo (CT) lakes in Europe and maps of their catchments with locations of low (L) and high (H) elevation throughfall plots (PL-L, PL-H, CT-L, and CT-H), bulk precipitation plots (BP), and additional research plots in the survived PL forest beneath living trees (LT) and beneath dead and broken trees (DT). Brown colour in the PL catchment denotes areas with dominant dead trees in 2000. Gray colour denotes catchment parts with dieback of the original forest stands after 2000: (1) in the PL catchment, >80% reduction of living trees by bark beetle infestation during autumn 2004–2018 (Kopáček et al. 2017); (2) in the CT catchment, >50% reduction of living trees by windthrows in 2007 and 2008 and the following bark beetle infestation (Kopáček et al. 2016). Water discharge from lakes was recorded at weirs.

Table SI-1. Locations of research plots for measurement of bulk precipitation (in treeless areas), throughfall, temperature and moisture in the Bohemian Forest. Abbreviations: PL, Plešné Lake; CT, Čertovo Lake; BP, bulk precipitation; L, low elevation; H, high elevation; DT, dead trees; LT, living trees; ND, not determined.

	PL catchment					CT catchment		
	BP	Throughfall		Temperature		BP	Throughfall	
	PL-BP	PL-L	PL-H	DT	LT	CT-BP	CT-L	CT-H
Latitude (°N)[1]	48.7760	48.7758	48.7773	48.7774	48.7777	49.1754	49.1627	49.1696
Longitude (°E)[1]	13.8708	13.8689	13.8556	13.8634	13.8632	13.1990	13.1993	13.1858
Elevation (m)	1087	1122	1334	1130	1143	1180	1057	1330
Precipitation[2]	1998–2018	1998–2018	2001–2018	ND	ND	1998–2018	1998–2018	1998–2017
Soil temperature (–0.05 m)[2,3]	ND	2004–2018	2004–2018	2014–2016	2014–2016	ND	2004–2018	2004–2017
Soil moisture[2]	ND	2008–2018	ND	ND	ND	ND	2008–2018	ND
Air temperature (0.3 m)[2,4]	ND	ND	ND	2012–2016	2012–2016	ND	ND	ND
Air temperature (2 m)[2,4]	ND	2004–2018	2004–2018	2012–2016	2012–2016	ND	2004–2018	2004–2017
Air humidity (2 m)[2,5]	ND	2009–2018	2009–2018	2012–2016	2012–2016	ND	2009–2018	2009–2017

[1]Data given in World Geodetic System (WGS-84).
[2]Data show periods of measurement.
[3]Themometers were situated 5 cm below ground in (or below) the litter horizon.
[4]Themometers were situated in solar radiation shields (diameter of 10 cm, height of 15 cm) fixed on northern sides of wooden poles 30 cm and 2 m above ground, respectively.
[5]Relative air humidity was measured at 2 m above ground.

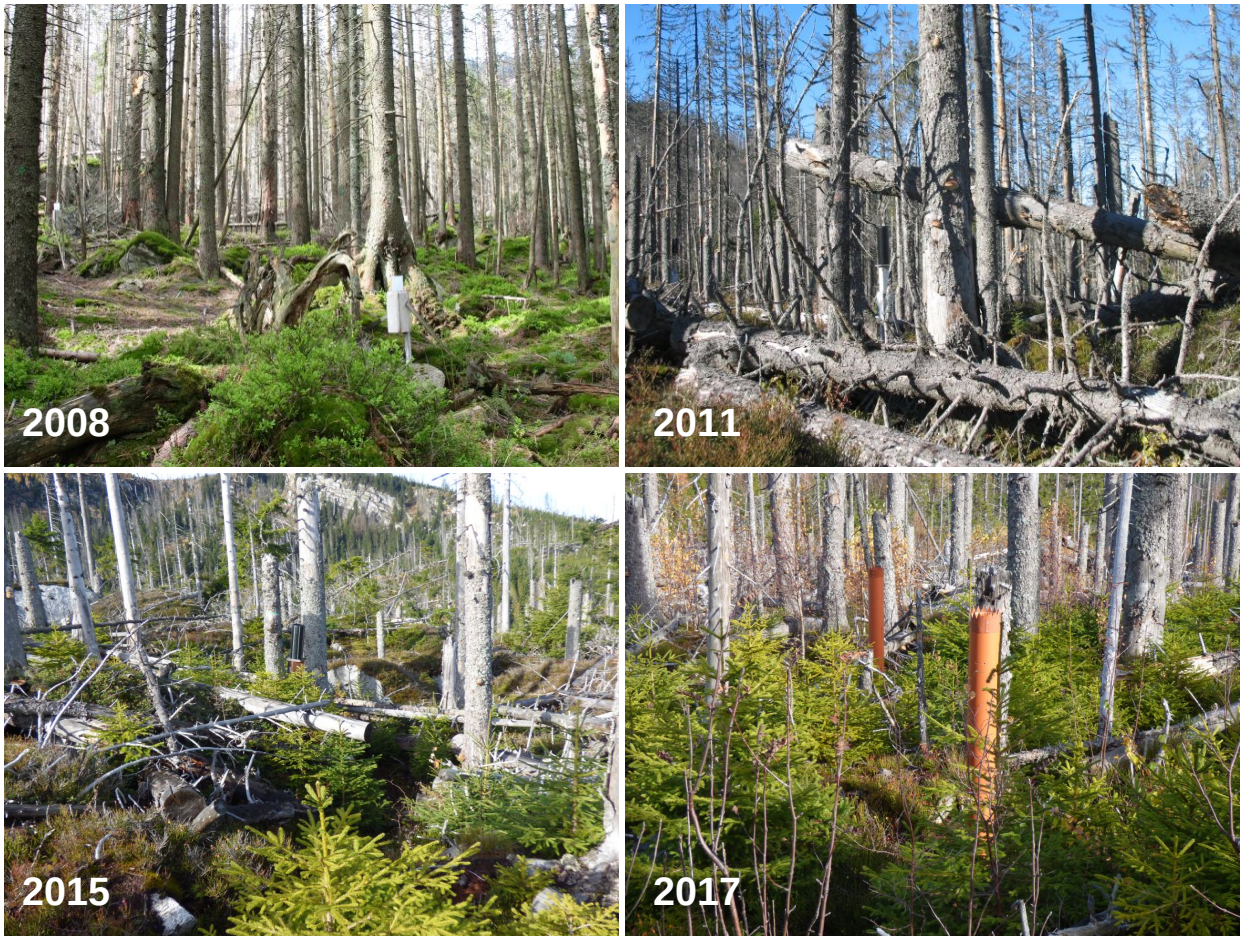

Fig. SI-2. Photographs of the low elevation plot in the Plešné catchment (PL-L) showing development of forest status one year after tree dieback (2008) and its development during the following years, with already abundant spruce seedlings and young rowan and birch trees in 2017. Photo: J. Kopáček.

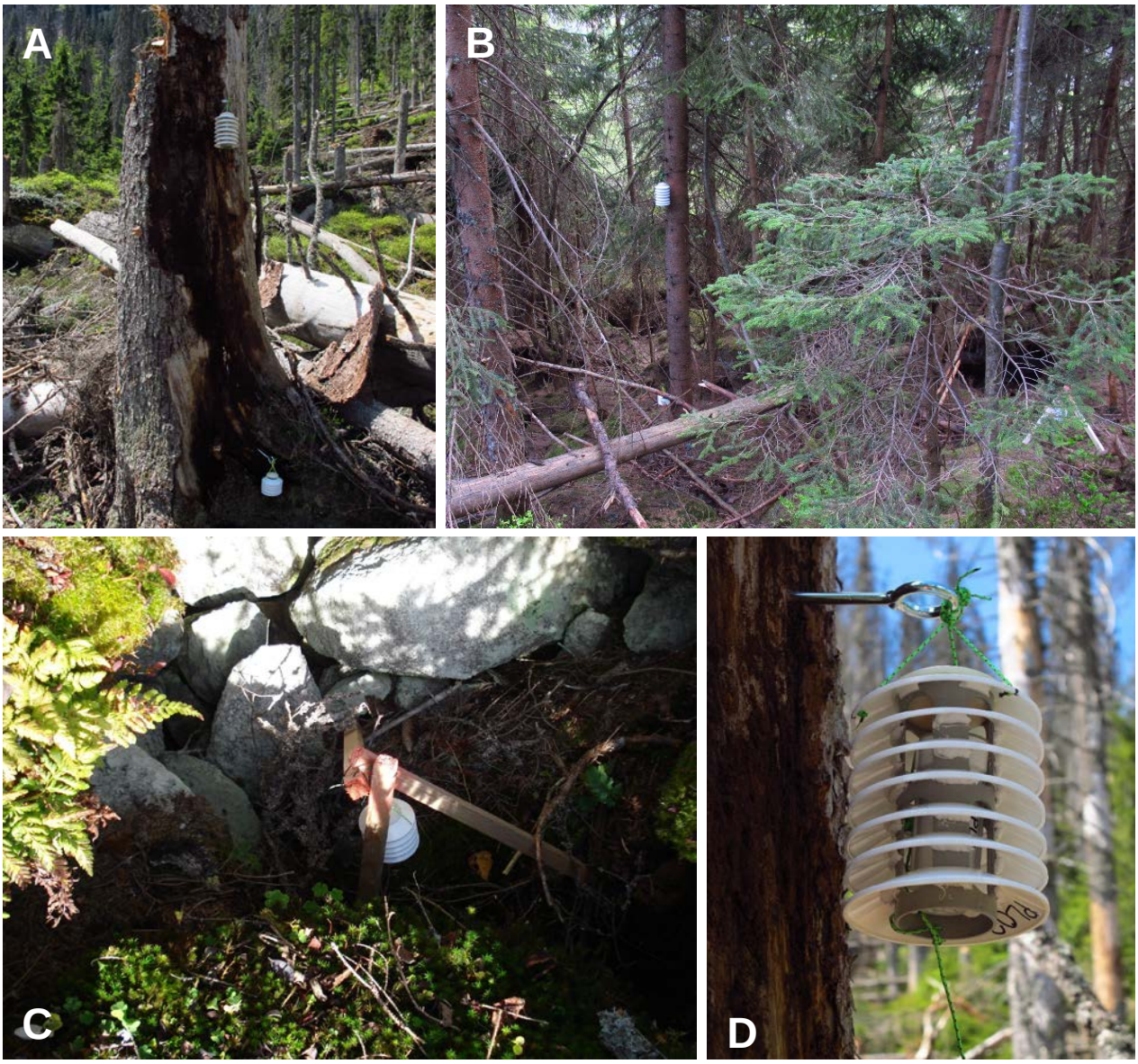

Fig. SI-3. Photographs of selected microhabitats at the DT (dead tree) and LT (living tree) plots in Plešné catchment in 2012: (A) and (B) central microhabitats at the DT and LT plots, respectively, with thermometers situated at 2 and 0.3 m above ground; (C) tripod with thermometer in natural depression between rocks at the DT plot, and (D) detail of solar radiation shields (diameter of 10 cm, height of 15 cm) fixed on northern side of trunk at the DT plot. Photo: T. Kučera.

Table SI-2. Number of mature and growing (young) trees (Norway spruce) and seedlings (diameter of canopy < 0.8 m) at the throughfall plots in the Bohemian Forest. Unit: number ha^{-1}. Data for 2000–2015 were calculated using colour aerial photographs (Kopáček et al. 2016, 2017), the 2018 data are based on direct counting in terrain (R. Bače, unpublished data).

Plot	Tree category	Year										
		2000	2003	2005	2007	2008	2009	2010	2011	2013	2015	2018
PL-L	Mature trees	709	701	661	64	48	0	0	0	0	0	0
	Growing trees	24	24	24	24	16	8	8	8	8	8	8
	Seedlings	0	0	0	0	0	0	0	72	119	422	1700
PL-H	Mature trees	709	709	231	104	88	8	8	8	8	0	0
	Growing trees	24	24	24	32	32	32	32	32	80	16	40
	Seedlings	0	0	0	0	0	0	48	80	223	350	760
LT	Mature trees	191	191	159	127	127	127	127	127	127	64	60
	Growing trees	318	318	318	318	318	318	318	318	478	414	520
	Seedlings	0	0	0	0	32	32	223	223	64	191	280
DT	Mature trees	299	252	133	44	37	3	3	3	3	0	0
	Growing trees	50	50	46	43	39	38	39	49	60	76	60
	Seedlings	14	23	51	69	82	90	137	185	357	570	1800
CT-L	Mature trees	307	ND	294	ND	287	ND	ND	285	ND	261	258
	Growing trees	45	ND	44	ND	43	ND	ND	40	ND	39	39
CT-H	Mature trees	312	ND	295	ND	245	ND	ND	229	ND	216	0
	Growing trees	123	ND	122	ND	113	ND	ND	104	ND	96	52

Table SI-3. Development of dominant understory vegetation in the Plešné (PL) and Čertovo (CT) catchments at the PL-L, PL-H, CT-L, and CT-H plots from 2007–2018 (Matějka 2015 and unpublished data). Units: g of dry weight biomass per m^2.

Plot	Tree category	Year											
		2007	2008	2009	2010	2011	2012	2013	2014	2015	2016	2017	2018
PL-L	*Avenella flexuosa*	6	2	0	0	1	1	1	1	6	6	0	1
	Vaccinium myrtillus	60	79	186	173	225	257	279	464	398	431	431	509
	Total	65	81	187	173	225	257	280	466	404	438	431	510
PL-H	*Avenella flexuosa*	27	29	52	67	92	103	108	108	142	151	136	108
	Calamagrostis villosa	34	37	66	56	51	32	33	55	55	58	51	55
	Luzula sylvatica	67	42	19	16	10	10	10	18	17	18	17	2
	Vaccinium myrtillus	90	97	101	85	189	201	201	111	54	58	178	272
	Total	218	205	237	224	342	347	352	291	268	285	381	436
CT-L	*Avenella flexuosa*	5	3	3	0	0	0	0	0	0	0	0	0
	Vaccinium myrtillus	284	116	127	208	212	188	188	188	175	200	244	264
	Total	289	119	130	208	212	188	188	188	176	200	244	264
CT-H	*Avenella flexuosa*	33	35	61	74	76	78	73	81	75	71	80	22
	Calamagrostis villosa	39	31	36	25	27	28	37	31	41	34	30	62
	Total	72	67	98	100	103	106	110	112	116	104	110	85

Part SI-2: Details to Materials and Methods

Section: Air temperature and humidity and soil temperature and moisture

Long-term trend in annual air temperature at the CT-L plot in the catchment of Čertovo Lake (Fig. SI-3) was reconstructed by Turek et al. (2014), using hourly measurements at the CT-L plot during 2004–2012 and their correlations with daily air temperatures back to 1961 and monthly mean air temperatures back to 1781 from Churáňov meteorological station (Bohemian Forest) and Hohenpeissenberg meteorological station (Germany), respectively. The meteorological station Churáňov (Czech Hydrometeorological Institute; 49.07 N, 13.61 E) is situated in the central part of the Bohemian Forest ~40 km southeast of Čertovo Lake and ~30 km northwest of Plešné Lake at elevation of 1118 m a.s.l. The data were recorded daily at 7, 14, and 21 hour from 1 January 1961 to 31 December 2012. The Hohenpeissenberg station is situated at 47.80 N, 11.01 E, and elevation of 977 m a.s.l. The data come from Global Historical Climatology Network, version 3 (Lawrimore et al. 2011) and were downloaded via the web page of www.ncdc.noaa.gov/ghcnm/v3.php. The data consist of monthly means from 1781 to 2012, with the exception of missing data from June 1862 to March 1864. The data from Hohenpeissenberg have been demonstrated to be robust and free of interference due to urbanisation or changes in instrumentation or position (Schönwiese 1987). The original data by Turek et al. (2015) were updated till 2018 using the same approach.

Part SI-3: Details to Results

Sections: "Between-catchment differences in air and soil temperature and relative air humidity" and "Between-plot differences in air and soil temperature and air humidity in the Plešné catchment"

Following Fig. SI-4A,B,C show details on trend analyses of air temperature given in Fig. 5 that include decomposing time series into three components (seasonality, trends, and random fluctuation) done in R environment for statistical computing (R Core Team 2019). The original time series (A) was split into seasonal patterns (B) that repeat with a fixed period of time, trend (C) that represents the underlying trend of the metrics, and random values (D) that show residuals of the original time series after the seasonal and trend series are removed. Trends shown in Fig. 6 and 7 were determined analogously.

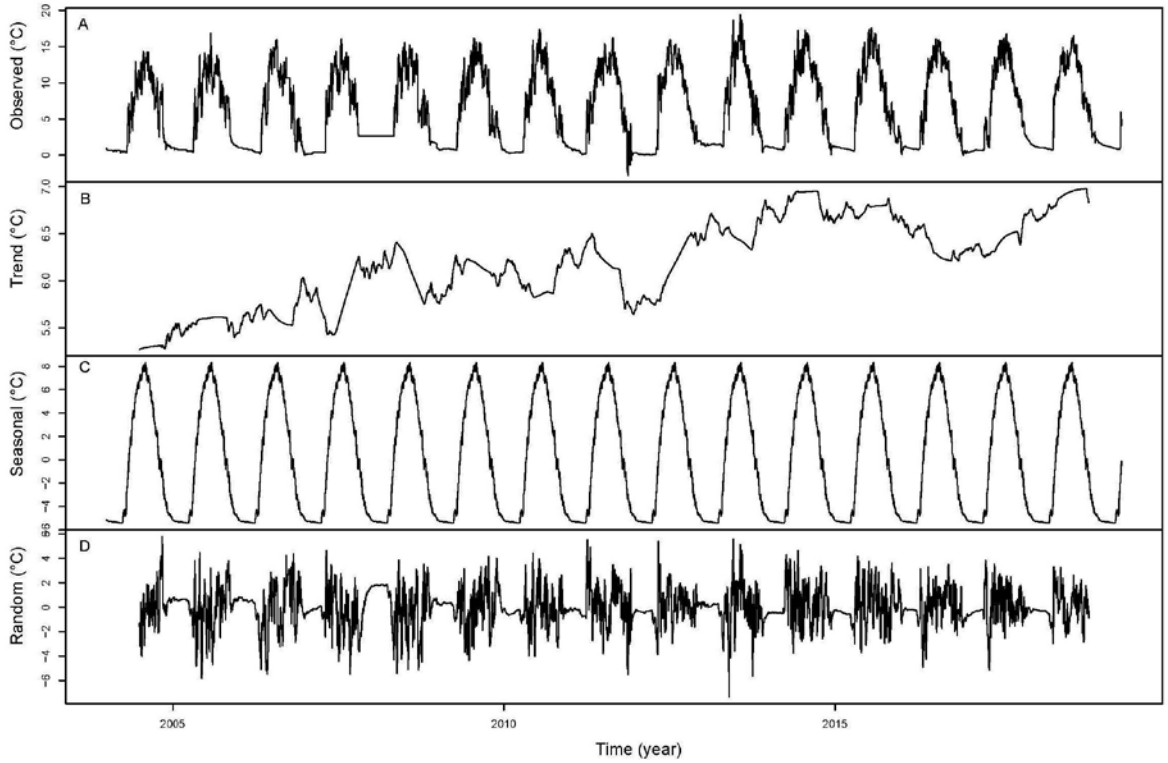

Fig. SI-4A. Decomposition of daily mean air temperature at the PL-L plot at 2 m above ground during 2004–2018 (A) into components of trend (B), seasonal periodical function (C), and random residuals (D).

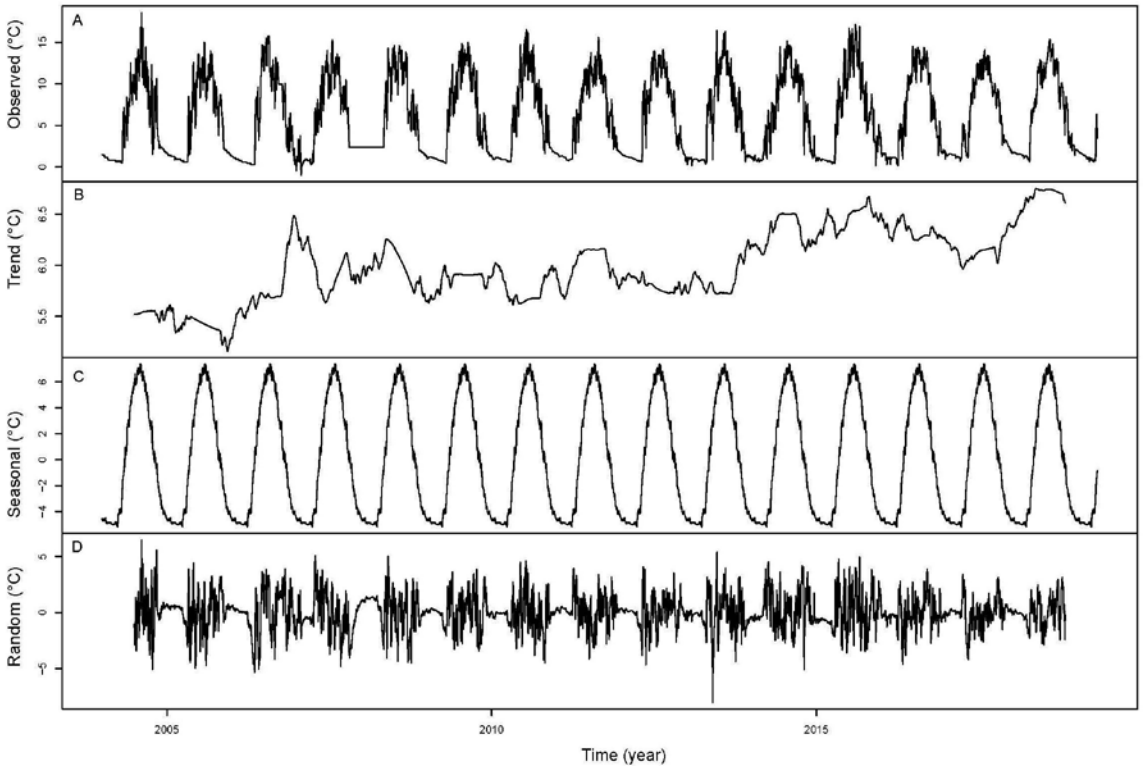

Fig. SI-4B. Decomposition of daily mean air temperature at the CT-L plot at 2 m above ground during 2004–2018 (A) into components of trend (B), seasonal periodical function (C), and random residuals (D).

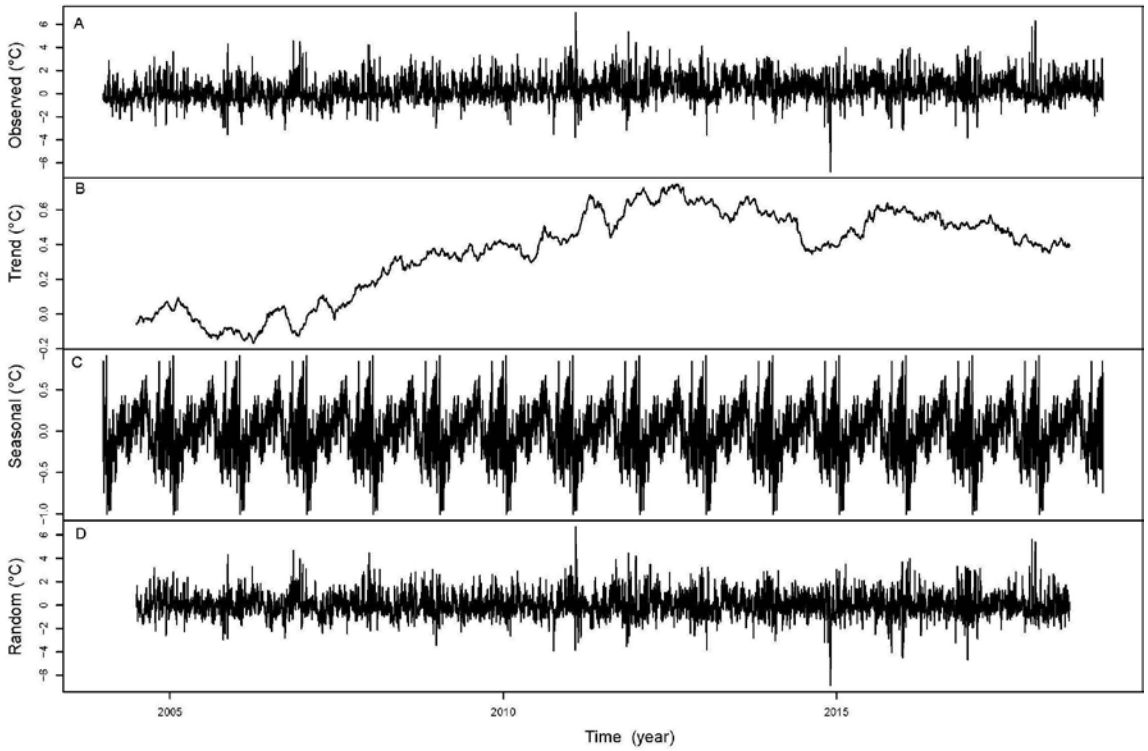

Fig. SI-4C. Decomposition of difference between daily mean air temperatures at the PL-L and CT-L plots at 2 m above ground (Δ PL-L–CT-L) during 2004–2018 (A) into components of trend (B), seasonal periodical function (C), and random residuals (D).

Table SI-4. The τ-values of seasonal Mann-Kendall test (R Core Team 2019) and rate of change of trends in soil and air temperature and relative air humidity at low (L) and high (H) elevation plots in catchments of Plešné (PL) and Čertovo (CT) lakes. For plot location and characteristics see Fig. SI-1 and Table SI-1. Rate of change is Sen's slope multiplied by number of days during particular period (365 days on annual basis and 214 days during growing season). Year 2018 was excluded due to tree dieback at the CT-H plot. Negative values of rate indicate decreasing trends. Significance: (***, $p < 0.001$; **, $p < 0.01$; *, $p < 0.05$; and NS, not significant).

Variable	Plot	Kendall's τ & Rate of change	Annual data				Growing season			
			Average	Minimum	Maximum	Amplitude	Average	Minimum	Maximum	Amplitude
Soil temperature (°C) at 0.05 m below ground (2004–2017 period)	PL-L	τ	0.055^{***}	0.013^{NS}	0.076^{***}	0.163^{***}	0.110^{***}	0.030^{*}	0.181^{***}	0.316^{***}
		Rate (°C yr^{-1})	0.050	0.009	0.069	0.038	0.097	0.022	0.188	0.123
	PL-H	τ	0.105^{***}	0.109^{***}	0.101^{***}	0.065^{***}	0.071^{***}	0.079^{***}	0.057^{***}	0.022^{NS}
		Rate (°C yr^{-1})	0.085	0.083	0.085	0.002	0.055	0.057	0.049	0.004
	CT-L	τ	0.046^{***}	0.042^{***}	0.048^{***}	0.075^{***}	0.059^{***}	0.057^{***}	0.056^{***}	0.046^{***}
		Rate (°C yr^{-1})	0.041	0.033	0.042	0.004	0.046	0.043	0.048	0.011
	CT-H	τ	0.043^{***}	0.034^{***}	0.048^{***}	0.100^{***}	0.079^{***}	0.062^{***}	0.092^{***}	0.135^{***}
		Rate (°C yr^{-1})	0.025	0.019	0.028	0.005	0.048	0.035	0.067	0.035
Air temperature (°C) at 2 m above ground (2004–2017 period)	PL-L	τ	0.053^{***}	0.037^{***}	0.073^{***}	0.128^{***}	0.060^{***}	0.030^{*}	0.091^{***}	0.147^{***}
		Rate (°C yr^{-1})	0.165	0.103	0.253	0.140	0.077	0.033	0.133	0.097
	PL-H	τ	0.046^{***}	0.043^{***}	0.068^{***}	0.089^{***}	0.048^{***}	0.037^{**}	0.074^{***}	0.089^{***}
		Rate (°C yr^{-1})	0.142	0.120	0.240	0.106	0.061	0.040	0.115	0.067
	CT-L	τ	0.038^{***}	0.038^{***}	0.034^{***}	0.001^{NS}	0.031^{*}	0.032^{**}	0.021^{NS}	-0.011^{NS}
		Rate (°C yr^{-1})	0.112	0.104	0.111	0.001	0.037	0.034	0.028	–0.006
	CT-H	τ	0.038^{***}	0.029^{**}	0.026^{**}	0.000^{NS}	0.030^{*}	0.030^{*}	0.018^{NS}	-0.014^{NS}
		Rate (°C yr^{-1})	0.112	0.079	0.084	0.000	0.038	0.032	0.025	–0.008
Relative air humidity (%) at 2 m above ground (2009–2017 period)	PL-L	τ	0.068^{***}	0.027^{*}	0.209^{***}	0.030^{**}	0.052^{***}	0.041^{**}	0.174^{***}	0.018^{NS}
		Rate (°C yr^{-1})	0.477	0.321	0.567	0.278	0.242	0.281	0.296	0.088
	PL-H	τ	0.059^{***}	0.011^{NS}	0.207^{***}	0.030^{*}	0.074^{***}	0.044^{**}	0.221^{***}	-0.002^{NS}
		Rate (°C yr^{-1})	0.339	0.079	0.366	0.212	0.258	0.273	0.181	0.000
	CT-L	τ	-0.023^{NS}	-0.018^{NS}	-0.034^{**}	0.011^{NS}	-0.051^{***}	-0.011^{NS}	-0.120^{***}	-0.019^{NS}
		Rate (°C yr^{-1})	–0.127	–0.167	–0.085	0.063	–0.190	–0.066	–0.175	–0.080
	CT-H	τ	0.004^{NS}	-0.009^{NS}	0.041^{***}	0.001^{NS}	0.022^{NS}	0.011^{NS}	0.090^{***}	-0.001^{NS}
		Rate (°C yr^{-1})	0.013	–0.073	0.088	0.000	0.073	0.059	0.104	0.000

Table SI-5. Average characteristics of air temperature (°C for all values) at 0.3 m above ground at 8 microhabitats differing in topographical and understory conditions at each of two neighbouring plots in the Plešné catchment with dead and broken trees (DT) and in the survived forest with living trees (LT) during 2012–2016. For plot locations see Fig. SI-1 and their other characteristics Tables SI-1 and SI-2.

Plot	Microhabitat description	Annual data					Growing season		
		Minimum	Maximum	Daily mean	Average minimum	Average maximum	Daily mean	Average minimum	Average maximum
Dead trees (DT)	Bare litter horizon	–12.4	38.3	7.4	3.9	12.8	11.4	7.1	18.1
	Dense young spruces	–13.4	33.4	6.6	3.6	10.6	10.6	6.7	15.6
	Depression between rocks	–11.6	26.5	5.8	4.1	8.5	9.3	7.2	12.9
	Dense old blueberry	–14.6	36.6	7.4	3.8	13.1	11.3	6.7	18.3
	Sparse raspberry	–15.0	38.3	6.5	3.4	12.0	10.7	6.4	18.3
	Young rowans	–14.5	36.2	7.3	3.7	12.5	11.4	6.7	18.0
	Below broken trunks	–9.1	36.4	6.8	3.9	11.3	10.5	6.6	16.7
	Fern	–13.9	39.9	7.4	4.0	13.4	11.3	6.7	19.0
Living trees (LT)	Bare litter horizon	–13.2	29.1	6.3	3.8	9.2	10.2	7.1	13.5
	Dense young spruces	–12.9	30.0	6.3	4.0	8.9	9.9	7.2	13.2
	Depression between rocks	–11.7	27.1	6.3	4.5	8.3	9.8	7.6	12.4
	Dense old blueberry	–13.6	31.0	6.5	4.0	9.6	10.2	7.0	13.9
	Sparse raspberry	–12.8	31.1	6.3	3.9	9.0	10.0	7.2	13.3
	Young rowans	–13.0	31.8	6.6	4.1	9.9	10.4	7.3	14.5
	Litter horizon with moss	–13.1	30.4	6.6	4.3	9.4	10.3	7.3	13.8
	Sparse young blueberry	–12.9	31.7	6.5	4.2	9.4	10.2	7.3	13.9

Part SI-4: Details to Discussion
Section: Air and soil temperature

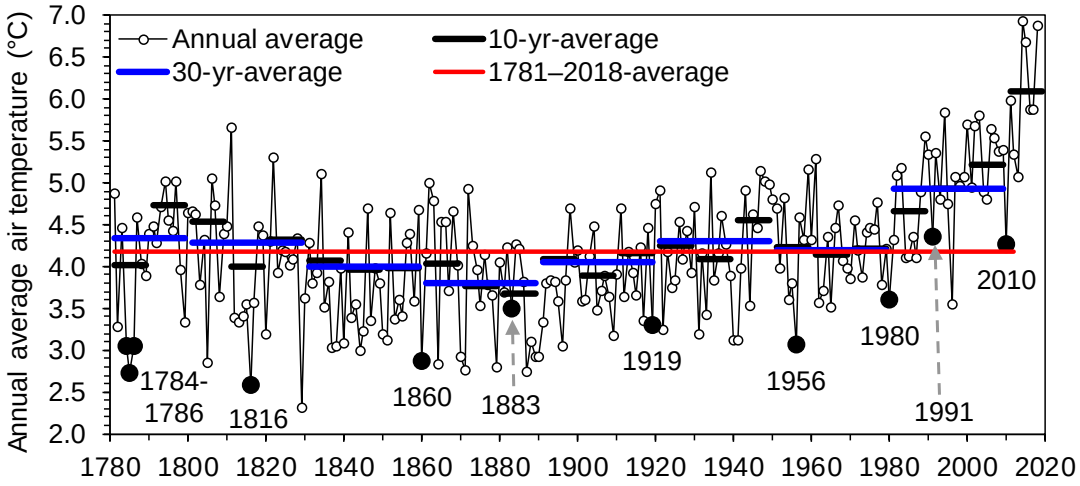

Fig. SI-5. The modelled trend in annual mean air temperature at the reference CT-L plot (2 m above ground). Legends: Individual values of annual average; and their averages for decades (10-yr-average), 3 decades (30-yr-average), and the whole 1781–2018 period (4.18 °C). Large black points indicate years with climate affected by volcanic eruptions. Date of eruption: Laki and Grímsvötn (1783–1785), Tambora (April 1815), Katla (May 1860, October 1918), Krakatau (August 1883), Bezymianny (March 1956), St. Helens (May 1980), Pinatubo (June 1991), and Eyjafjallajökull (May 2010). Data were updated from Turek et al. (2014).

Additional references

Lawrimore, J.H., Menne, M.J., Gleason, B.E., Williams, C.N., Wuertz, D.B., Vose, R.S., Rennie, J., 2011. An overview of the Global Historical Climatology Network Monthly Mean Temperature Data Set, Version 3. Journal of Geophysical Research, 116: D19121, doi:10.1029/2011jd016187.

Schönwiese, C.-D., 1987. Moving spectral analysis and some applications on long air temperature series. Journal of Climate and Applied Meteorology, 26, 1723–1730.